C_T, pH and A_T in the Canary Current Upwelling System

ESTOC

Mauritanian upwelling

Canary Region

CO_2

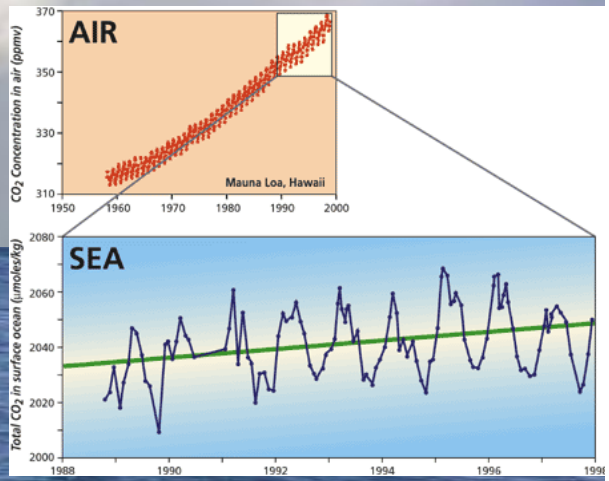

Ocean acidification

J. MAGDALENA SANTANA-CASIANO

Grupo QUIMA, IOCAG, ULPGC

TRAINING WORKSHOP IN THE CANARY CURRENT EASTERN BOUNDARY UPWELLING SYSTEM

IOC-UNESCO, Cabo Verde, 10-12 March 2020

Index

CO_2 and pH

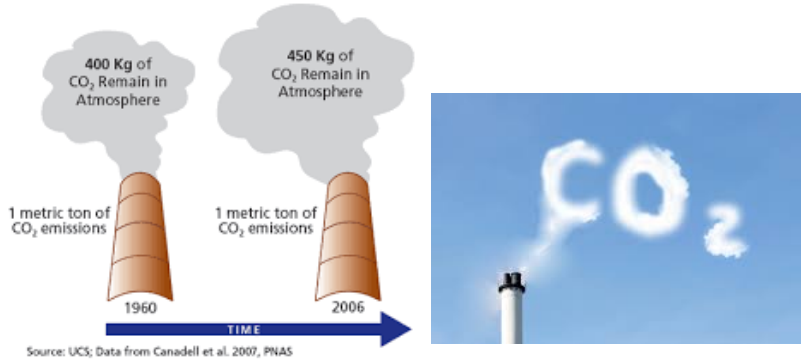
400 Kg of CO_2 Remain in Atmosphere
450 Kg of CO_2 Remain in Atmosphere
1 metric ton of CO_2 emissions
1 metric ton of CO_2 emissions
1960
2006
TIME
Source: UCS; Data from Canadell et al. 2007, PNAS

CO_2

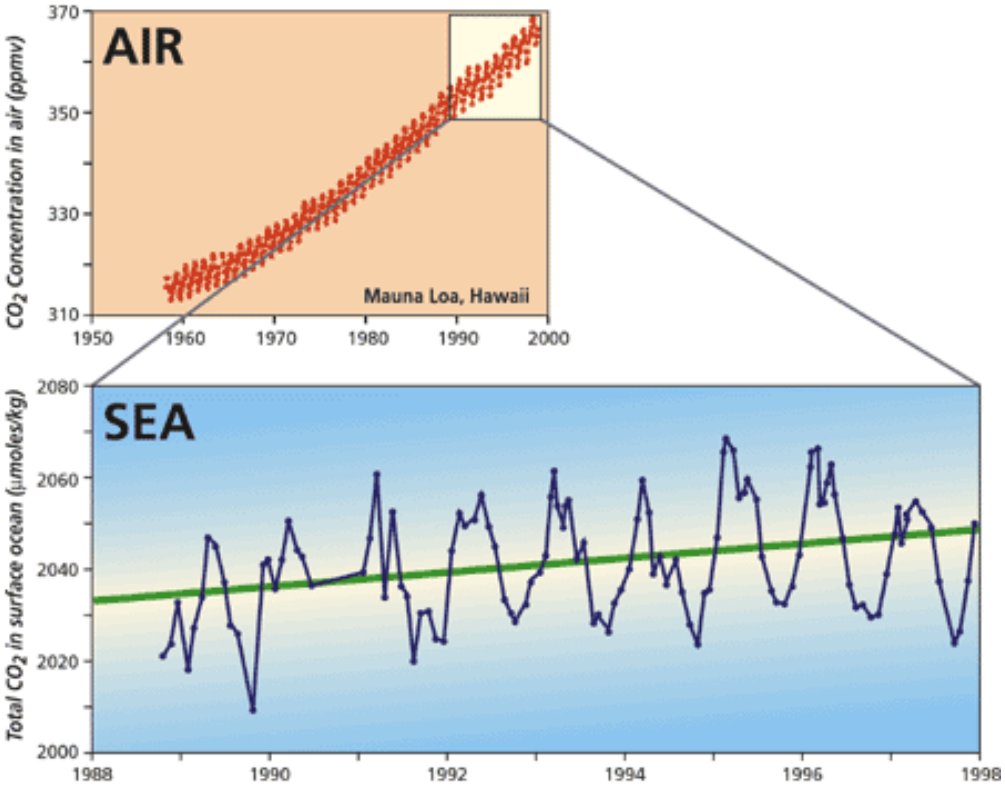
AIR
CO_2 Concentration in air (ppmv)
370
350
330
310
1950
1960
1970
1980
1990
2000
Mauna Loa, Hawaii
SEA
Total CO_2 in surface ocean (µmoles/kg)
2080
2060
2040
2020
2000
1988
1990
1992
1994
1996
1998

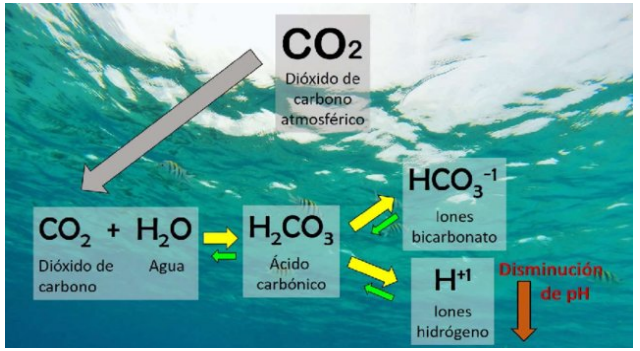
CO_2
Dióxido de carbono atmosférico
CO_2 + H_2O
Dióxido de carbono
Agua
H_2CO_3
Ácido carbónico
HCO_3^{-1}
Iones bicarbonato
H^{+1}
Iones hidrógeno
Disminución de pH

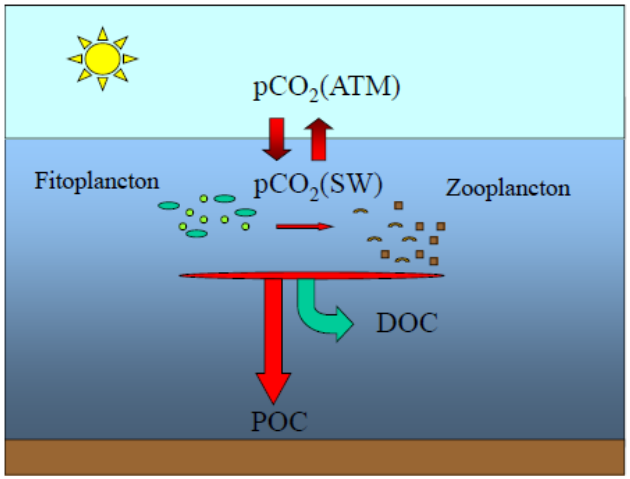
pCO_2(ATM)
Fitoplancton
pCO_2(SW)
Zooplancton
DOC
POC

CO_2 and pH

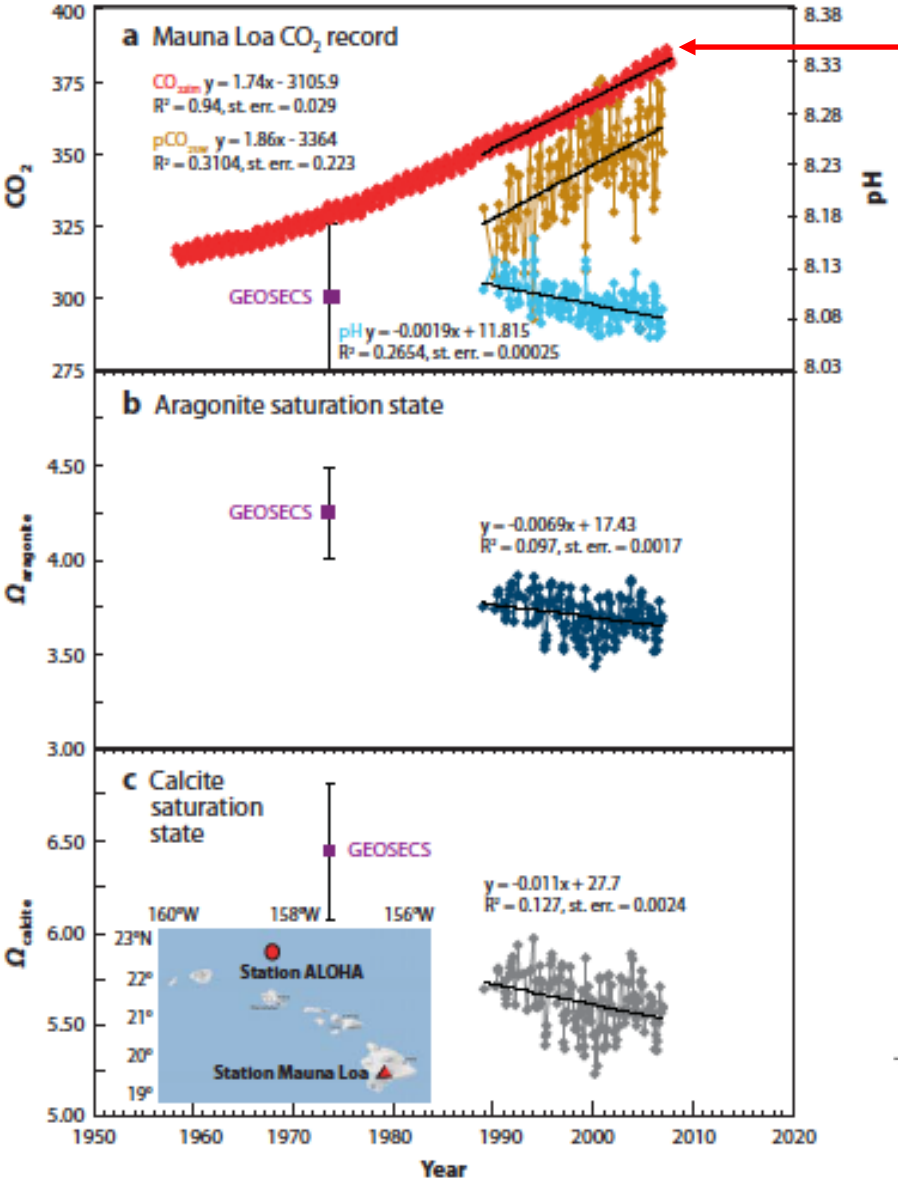

(Doney et al., 2008)

The oldest direct measurements of CO_2 in the atmosphere, in the Mauna Loa Station, Hawaii

Saturation state

$\Omega = [Ca^{2+}][CO_3^{2-}]$

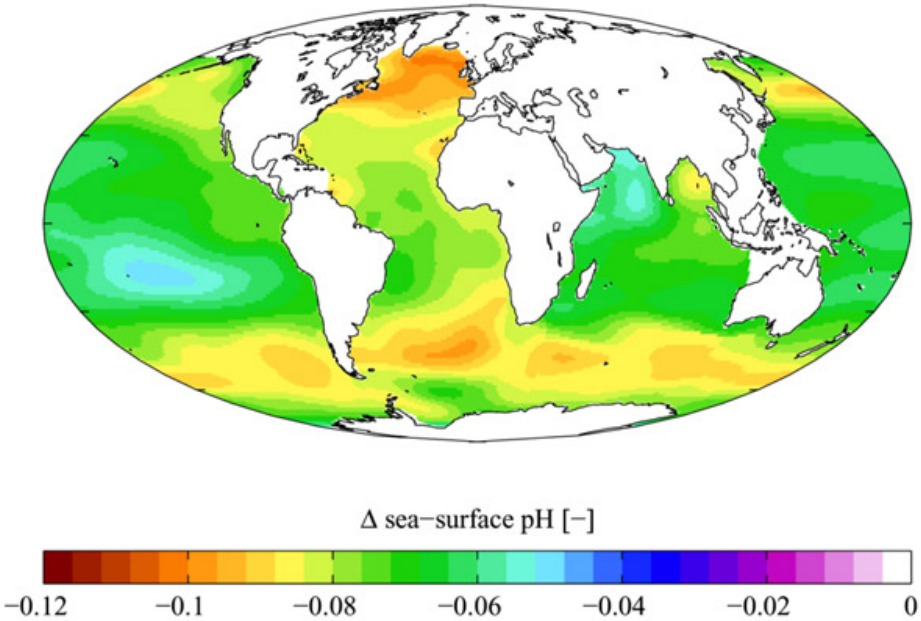

Changes in sea surface pH , 1700s – 1990

pH changes - Model predictions

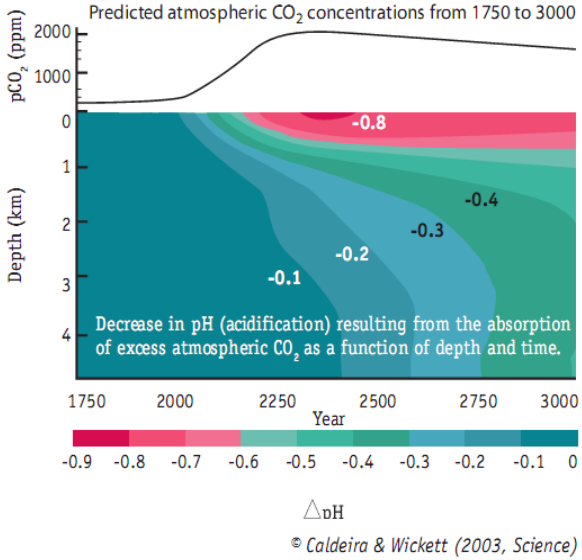

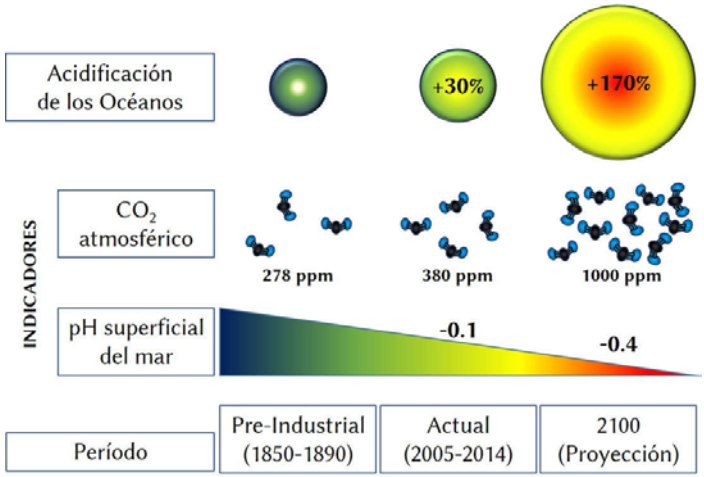

Castillo-Briceno et al., 2015

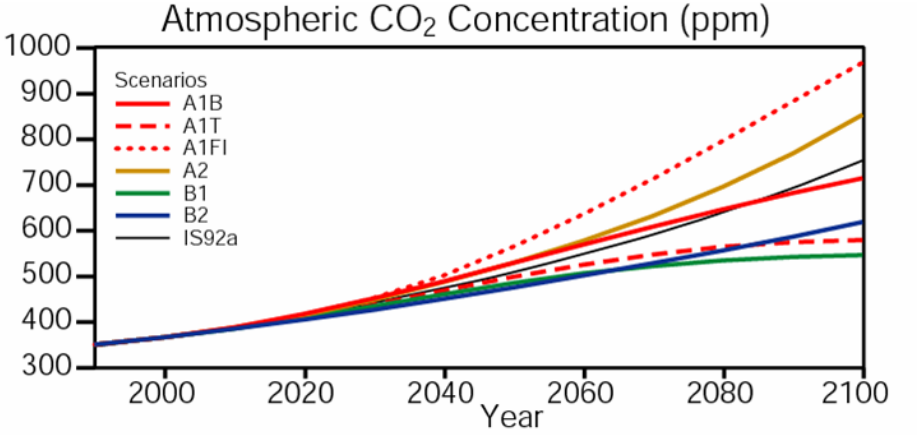

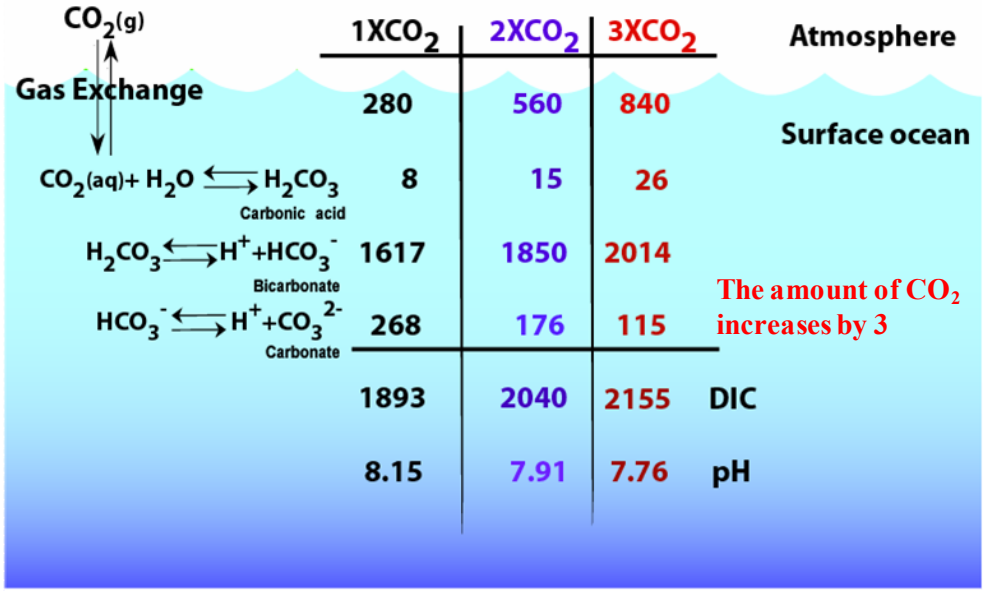

(Fabry et al., 2008)

The oceanic uptake of CO_2 after pre-industrial times has led to a reduction of the surface seawater pH of 0.1 units ➔ **30% increase in acidity**

Global Fossil CO_2 Emissions

Global fossil CO_2 emissions: 36.2 ± 2 $GtCO_2$ in 2017, 63% over 1990

● Projection for 2018: 37.1 ± 2 $GtCO_2$, 2.7% higher than 2017 (range 1.8% to 3.7%)

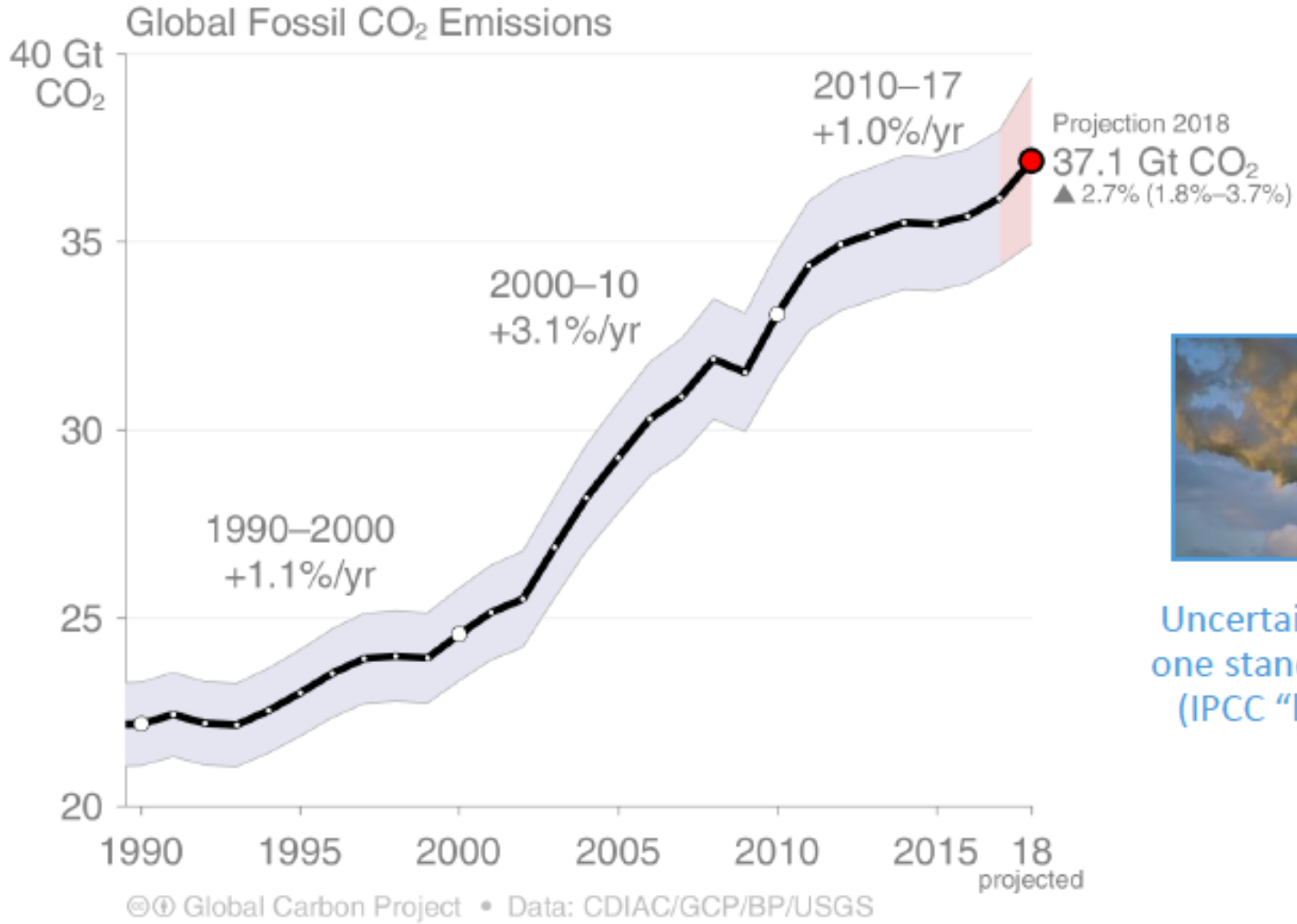

Uncertainty is ±5% for one standard deviation (IPCC "likely" range)

Estimates for 2015, 2016 and 2017 are preliminary; 2018 is a projection based on partial data.

Source: CDIAC; Le Quéré et al 2018; Global Carbon Budget 2018

Fate of anthropogenic CO_2 emissions (2008–2017)

Sources = Sinks

34.4 $GtCO_2/yr$

87%

combustion of fossil

13%

5.3 $GtCO_2/yr$

deforestation

17.3 $GtCO_2/yr$

44%

29%

11.6 $GtCO_2/yr$

22%

8.9 $GtCO_2/yr$

Budget Imbalance:
(the difference between estimated sources & sinks)

5%
1.9 $GtCO_2/yr$

Source: CDIAC; NOAA-ESRL; Houghton and Nassikas 2017; Hansis et al 2015; Le Quéré et al 2018; Global Carbon Budget 2018

Shared Socioeconomic Pathways (SSPs)

As a consequence of the C emissions, the temperature in the Earth is increasing

The curves in colours represent different scenarios of emissions and their effect in the increase of T at the end of this century. **The dot in black** are the real emissions

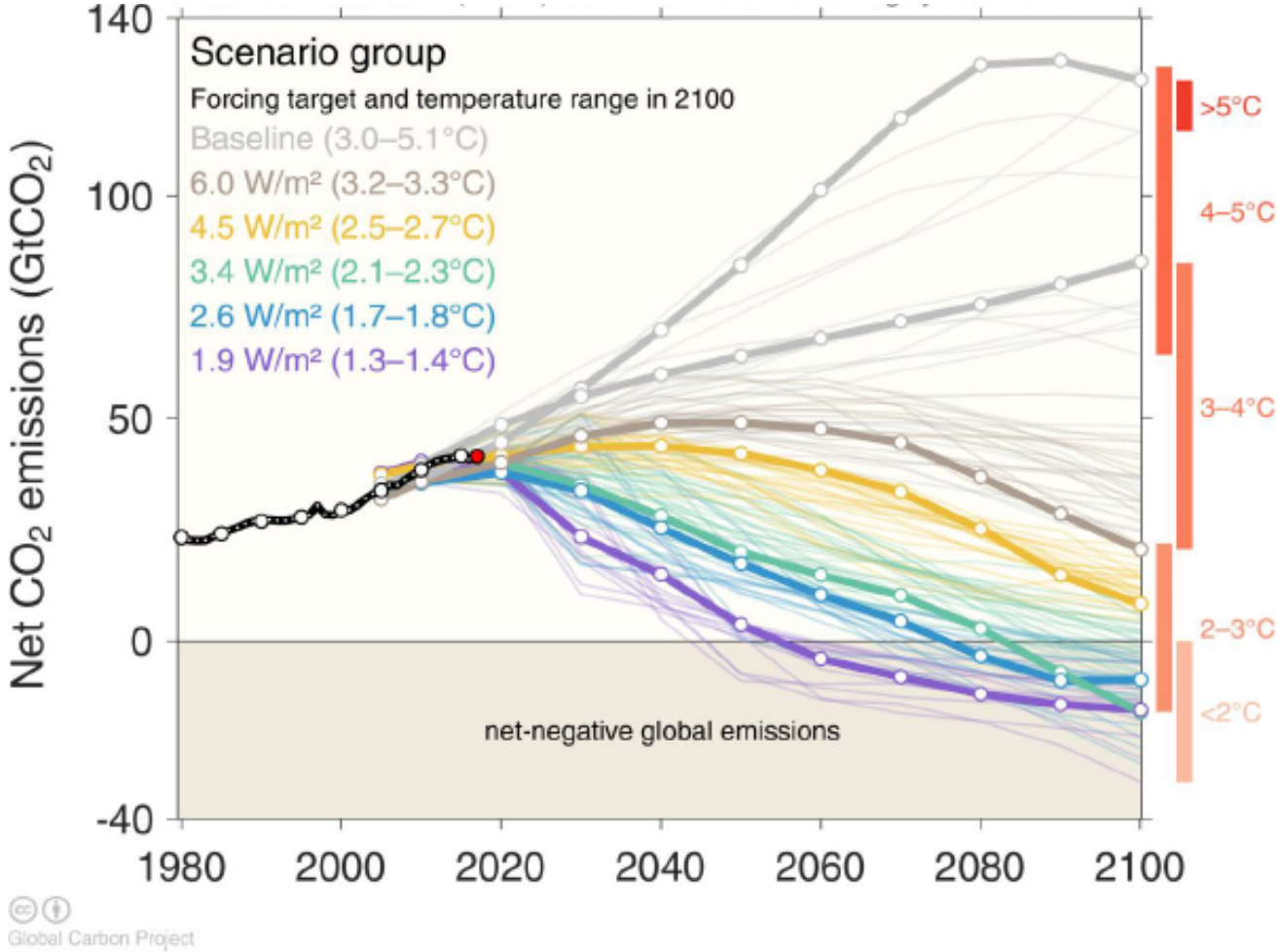

This set of quantified SSPs are based on the output of six Integrated Assessment Models (AIM/CGE, GCAM, IMAGE, MESSAGE, REMIND, WITCH). Net emissions include those from land-use change and bioenergy with CCS.

Source: Riahi et al. 2016; Rogelj et al. 2018; IIASA SSP Database; IAMC; Global Carbon Budget 2018

CO2 equilibria

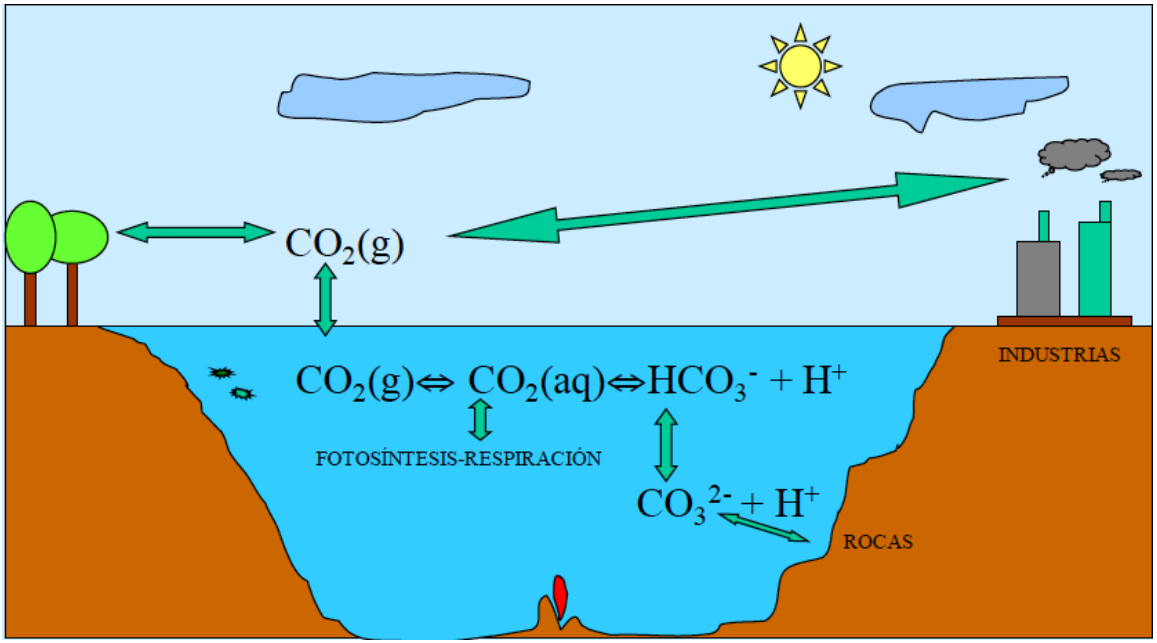

$$CO_{2(g)} \Leftrightarrow CO_{2(aq)} \qquad K_0 \ (1)$$

$$CO_{2(aq)} + H_2O \Leftrightarrow HCO_3^- + H^+ \qquad K_1 \ (2)$$

$$HCO_3^- \Leftrightarrow CO_3^{2-} + H^+ \qquad K_2 \ (3)$$

$$Ca^{2+} + CO_3^{2-} \Leftrightarrow CaCO_{3(s)} \qquad K_{sp} \ (4)$$

$$CO_2 + H_2O \Leftrightarrow CH_2O + O_2 \qquad (5)$$

Carbonate speciation as a function of the pH

At pH =8, the most important species is the $\mathbf{HCO_3^-}$

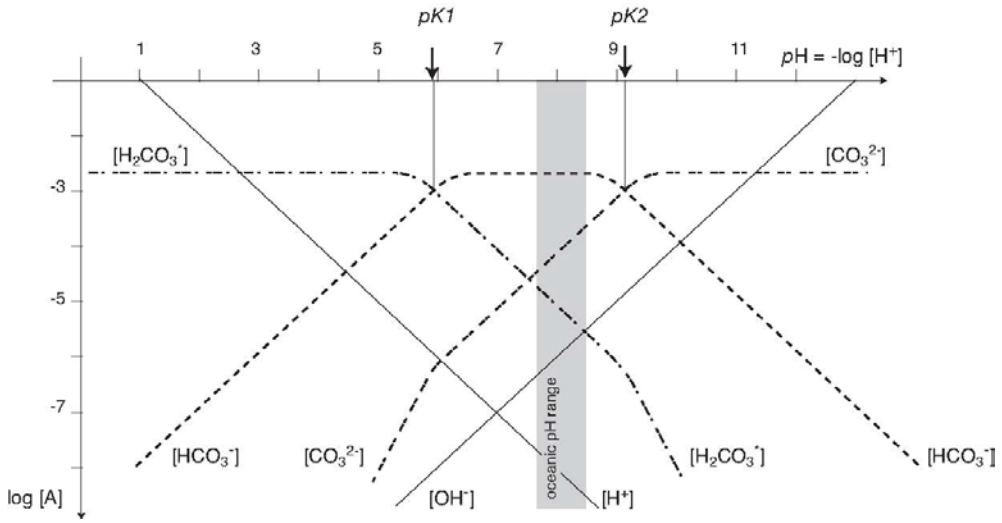

Pumps and Global Oceanic Circulation

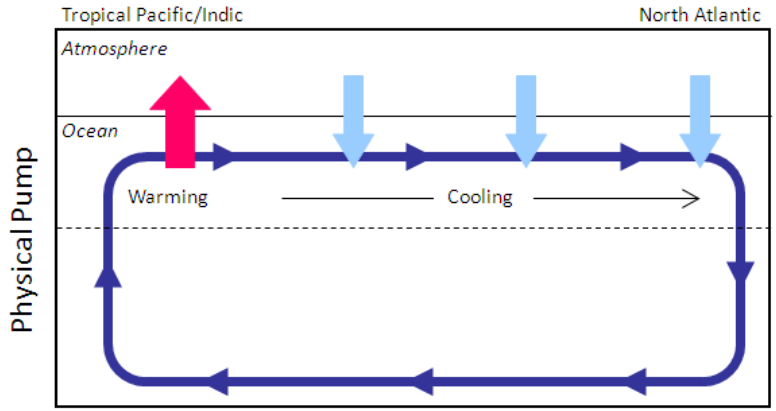

Solubility pump (Physical pump)

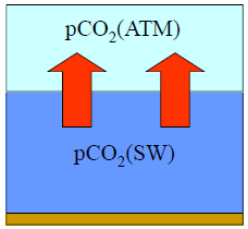

$$CO_{2(g)} \Leftrightarrow CO_{2(aq)}$$

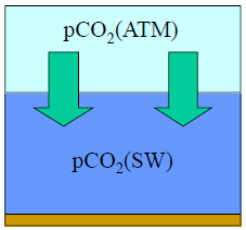

$$FCO_2 = 0.24 \cdot k \cdot s \cdot (fCO_2^{sw} - fCO_2^{atm})$$

$$k = (0.222 \cdot W^2 + 0.333 \cdot w) \cdot (Sc/660)^{-1/2},$$

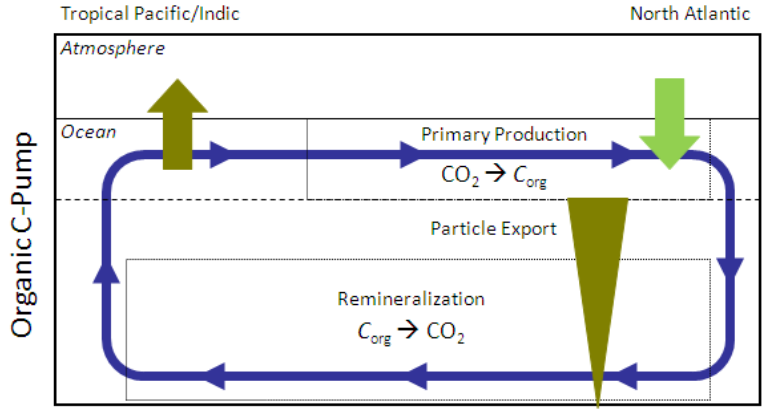

Biological pump (organic carbon)

$$CO_2 + H_2O \Leftrightarrow CH_2O + O_2$$

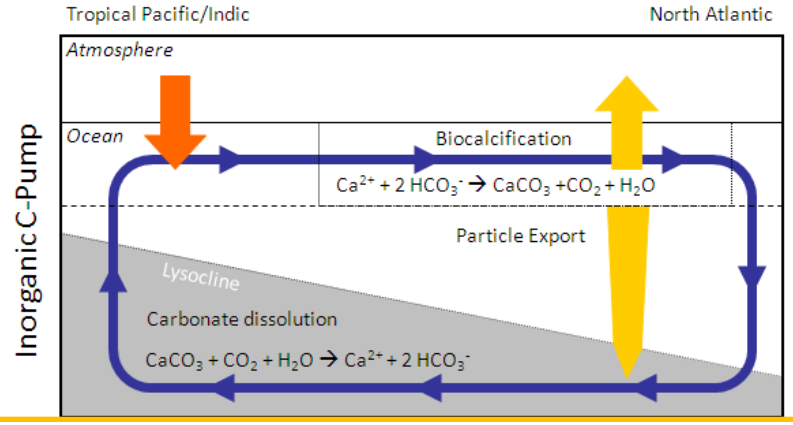

Carbonate pump
Biological pump, inorganic carbon)

$$CaCO_{3(s)} \Leftrightarrow Ca^{2+} + CO_3^{2-}$$

THC and seasonal mixing

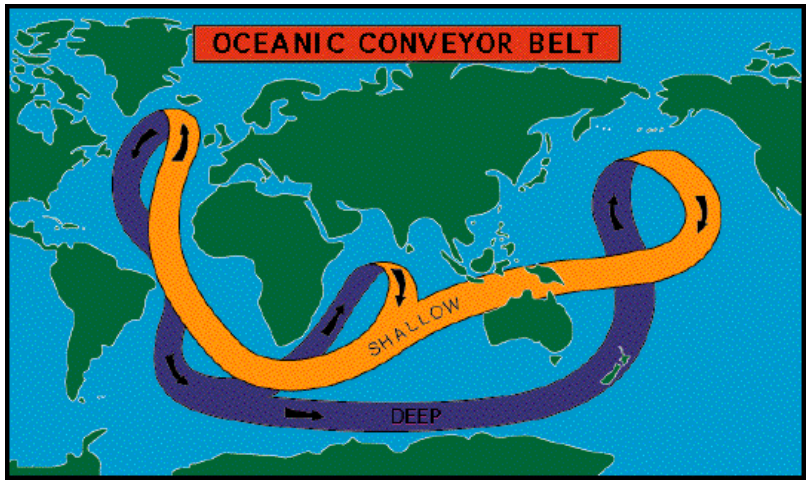

The **thermohaline circulation** and the **seasonals changes in the MLD** explain CO_2 entrance to the surface waters and also the content of CO_2 in the different basins

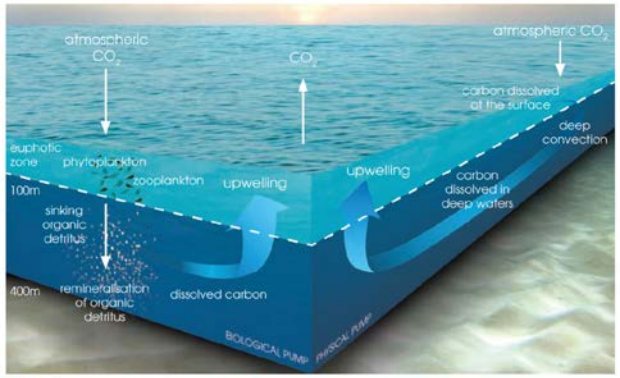

Fig. 1— Natural carbon cycle and representation of biological and physical pumps (Bopp *et al.* 2002).

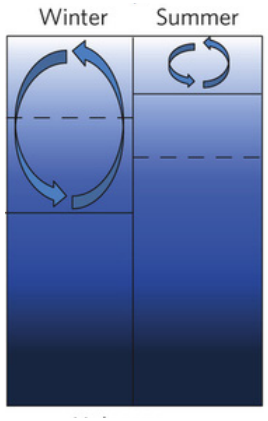

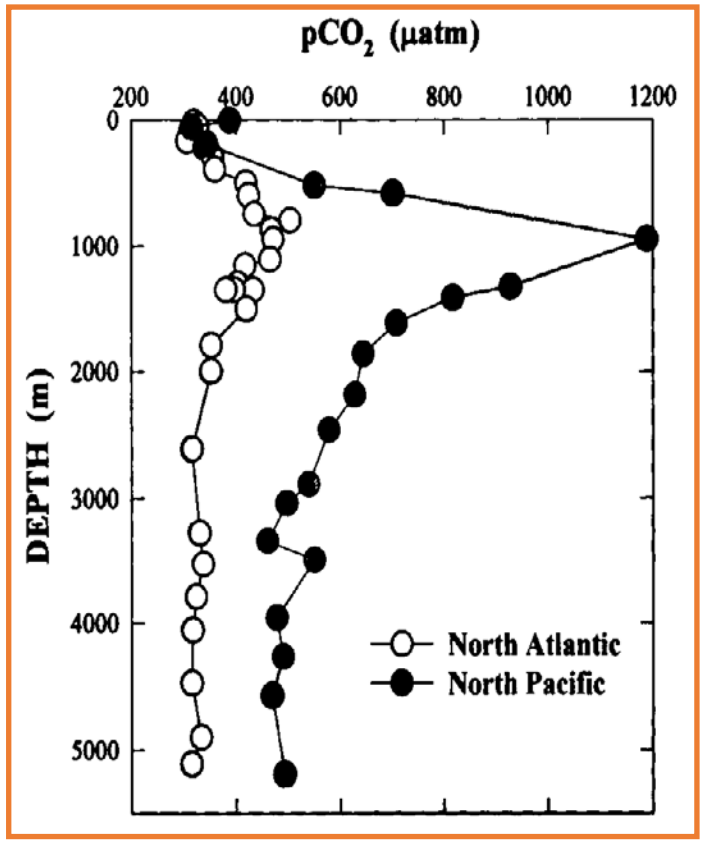

Pacific waters are more concentrated in CO_2 than Atlantic because they are older due to the THC, higher remineralisation

Measurable CO2 parameters

Partial pressure of CO_2 or fCO_2

$$pCO_2 = \frac{[CO_2^*(aq)]}{K_H}$$

fCO_2 when CO_2 is considered a real gas and interactions between CO_2-H_2O molecules are taken into account

Total dissolved inorganic carbon (DIC, C_T, TCO_2, ΣCO_2)

0.5% 88.6% 10.9%

$$C_T = [CO_2^*] + [HCO_3^-] + [CO_3^{2-}] = [CO_2] + [H_2CO_3] + [HCO_3^-] + [CO_3^{2-}]$$

Total alkalinity (TA, A_T)

76.8% 18.8% 4.2% 0.2%

$$A_T = [HCO_3^-] + 2[CO_3^{2-}] + [B(OH)_4^-] + [OH^-] + [HPO_4^{2-}] + 2[PO_4^{3-}] + [SiO(OH)_3^-] + [NH_3] + [HS^-] + \ldots$$
$$- [H^+] - [HSO_4^-] - [HF] - [H_3PO_4]$$

pH

$$pH = -\log[H^+]$$

Vertical profiles

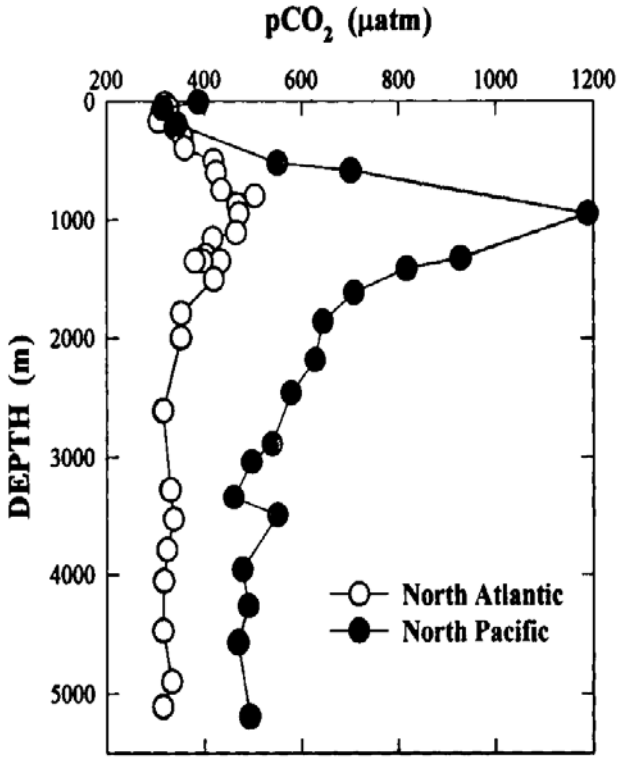

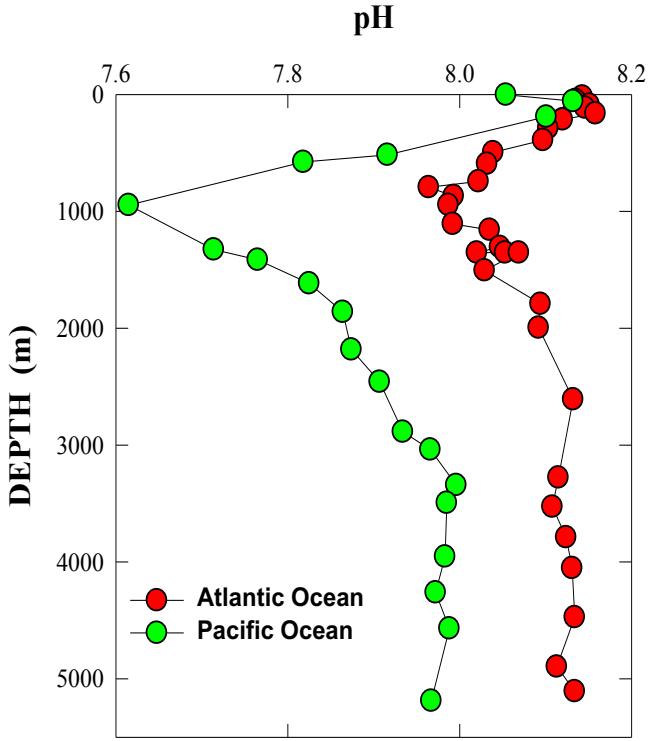

pCO_2 Low surface values due to photosynthesis
High values at 1000m due to the greater remineralization at this depth

Pacific waters are **more concentrated in pCO_2 and acid** than Atlantic because they are older due to the THC and higher remineralisation

Vertical profiles

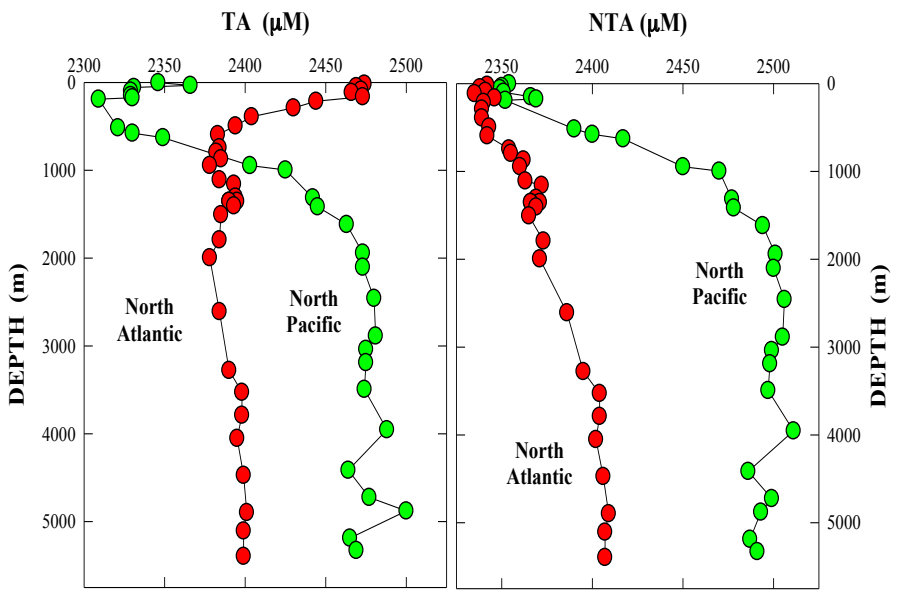

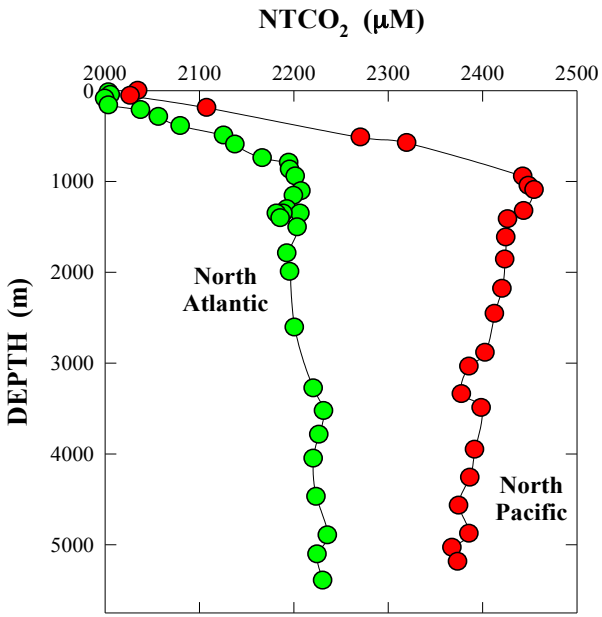

A_T The surface waters of the Atlantic have higher alkalinity than those of the Pacific due to their higher salinity.

NA_T To correct the effect of salinity, alkalinity is normalized

$$NA_T = A_T x \frac{35}{S}$$

Processes that affect to the CO_2 system in the ocean

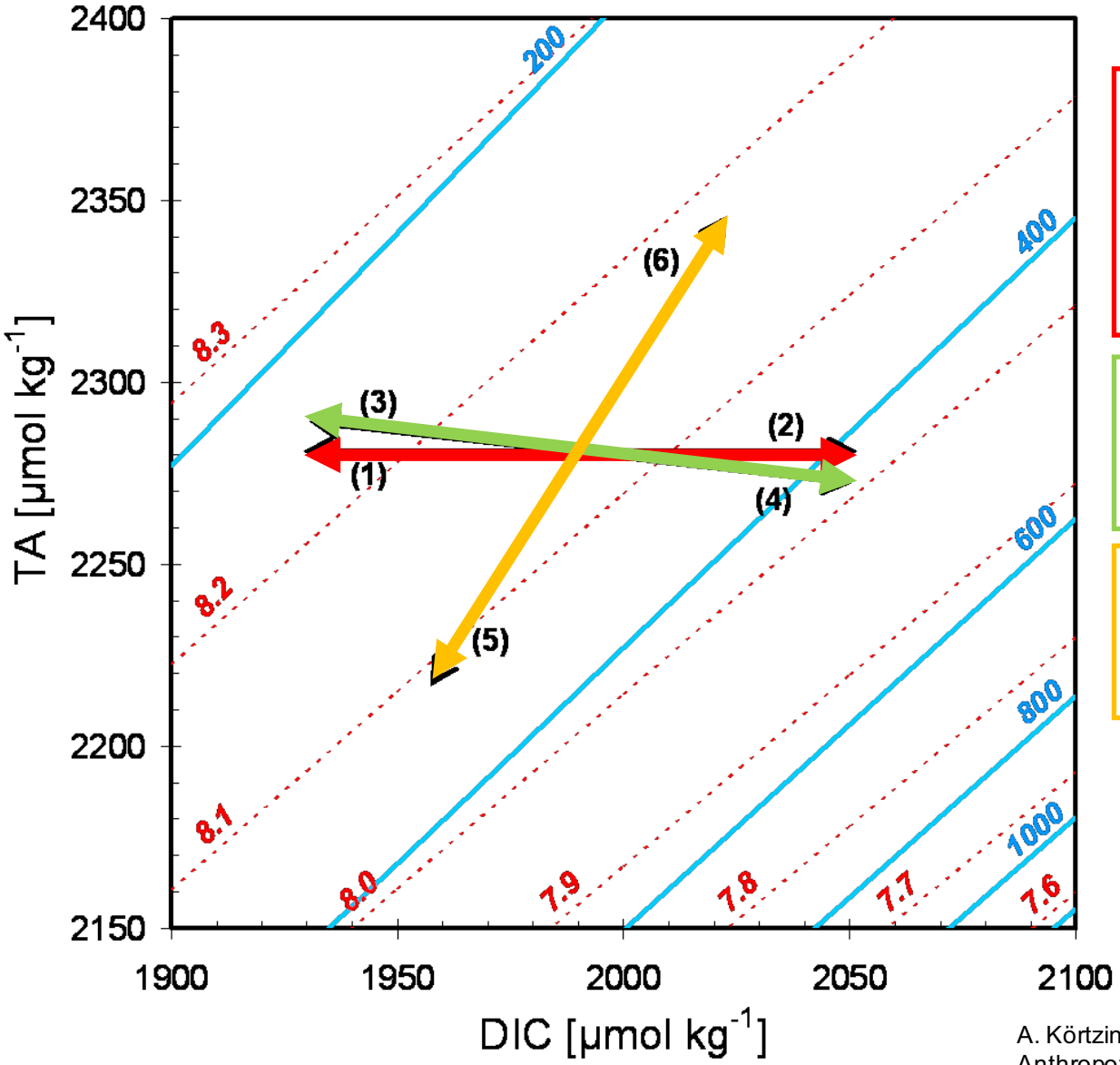

(1) Release of CO2 into the atmosphere

(2) CO_2 uptake by the ocean

(3) Primary production

(4) Respiration

(5) Calcification

(6) Carbonate dissolution

A. Körtzinger, Der globale Kohlenstoffkreislauf im Zeitalter des Anthropozäns – eine Betrachtung aus meereschemischer Perspektive, *Chemie in unserer Zeit*, 2/2010

Measurable parameters of the marine CO_2 system – accuracy/precisions

Table 8. Estimates of the Analytical Precision and Accuracy of Measurements of pH, TA, TCO_2, and pCO_2

analysis	precision	accuracy	ref
pH (spectrophometric)	±0.0004	±0.002	42
TA (potentiometric)	±1 μmol kg^{-1}	±3 μmol kg^{-1}	29
TCO_2 (coulometric)	±1 μmol kg^{-1}	±2 μmol kg^{-1}	96
f_{CO_2} (infrared)	±0.5 μatm	±2 μatm	97

From the measurements of two of the parameters, the other two can be determined

Table 9. Estimated Probable Errors in the Calculated Parameters of the Carbonate System Using Various Input Measurements

input	pH	TA (μmol kg^{-1})	TCO_2 (μmol kg^{-1})	f_{CO_2} (μatm)
pH−TA			±3.8	±2.1
pH−TCO_2		±2.7		±1.8
pH−f_{CO_2}		±21	±18	
f_{CO_2}−TCO_2	±0.0025	±3.4		
f_{CO_2}−TA	±0.0026		±3.2	
TA−TCO_2	±0.0062			±5.7

Millero, F.J., *Chemical Reviews* 107, 2007

Difference between accuracy and precision

Precision (Reproducibilidad)

Accuracy (Certeza, Precisión)

Precise
but not accurate

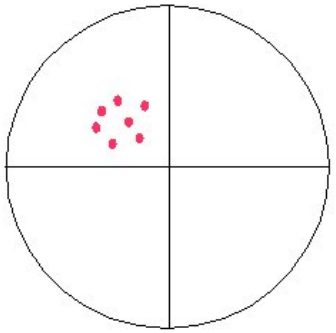

You can repeat a measurement several times and get the same values (reproducibility)

but this does not mean the value be correct (accurate).

Precise
and accurate

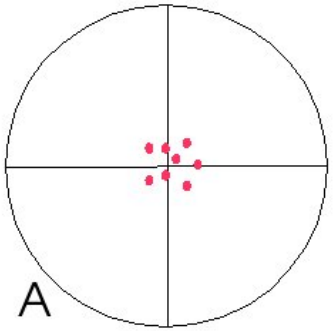

A

The accuracy is calculated using certified reference material or standard gases for pCO_2

Methodology

Research vessels

Mooring: Fixed point Observatories
Open Ocean
Coastal area

VOS lines: Observations from a 'Voluntary Observing Ship'

Methodology

Research vessels

Direct measurements of pH, A_T, C_T, continuos pCO_2

pH-potentiometric

pH-spectrophotometric

SP101-LB High Accuracy Lab / On ship pH sensor

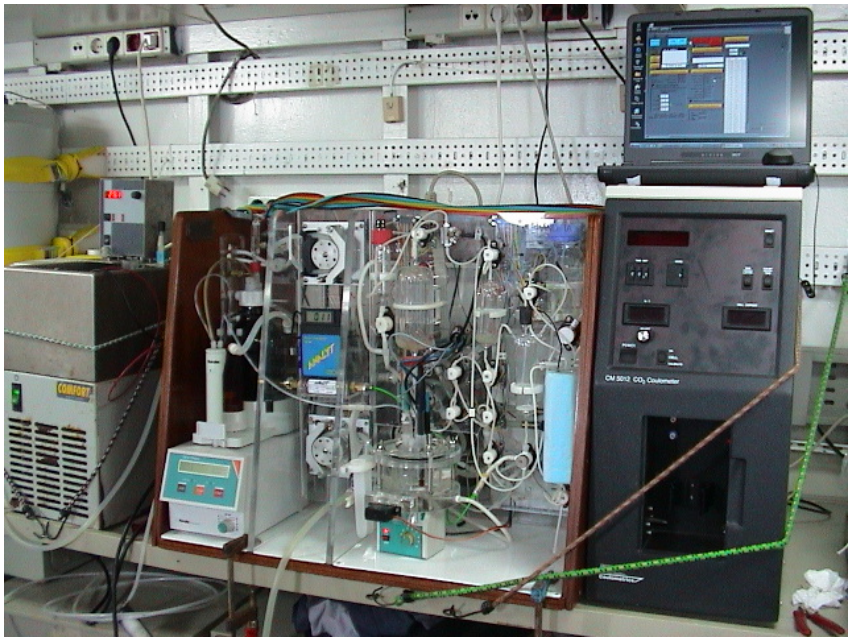

VINDTA system: A_T y C_T

Methodology

Mooring: Fixed point Open Ocean Observatories

A buoy with T, S, pCO_2 and pH sensors

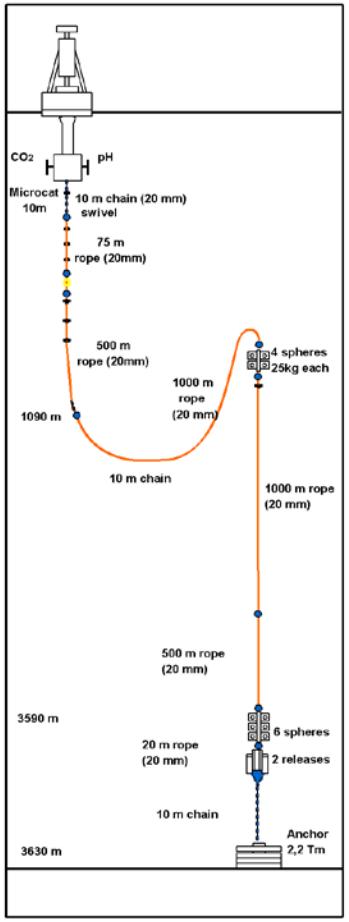

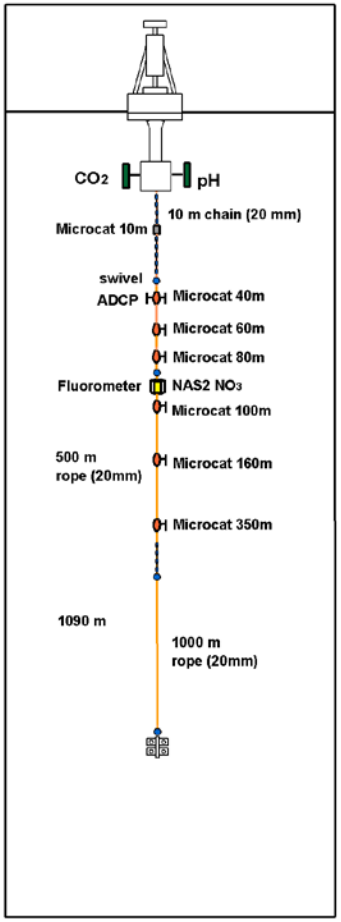

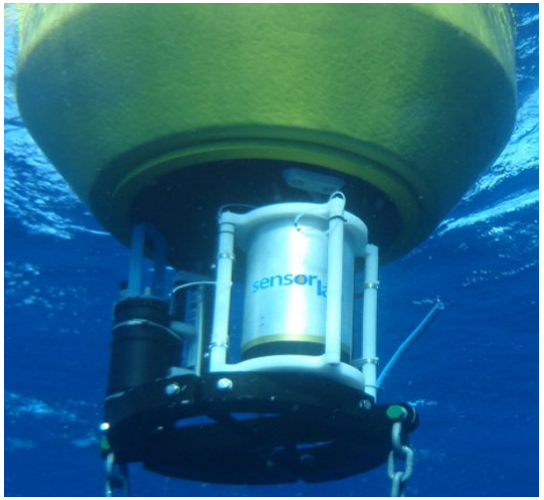

pH and pCO2 sensors

SP101-SM High accuracy Submarine pH sensor

Methodology

VOS lines: Observations from a 'Voluntary Observing Ship'

QUIMA-VOS line, was set up within the framework of:

- CARBOOCEAN Project (Marine carbon sources and sinks assessment) from July 2005 to 2010

- CARBOCHANGE Project (Changes in Carbon uptake and emission by oceans in a changing climate) from 2011 to 2015.

- ATLANTOOS 2017-2018

- CanOA, January 2019

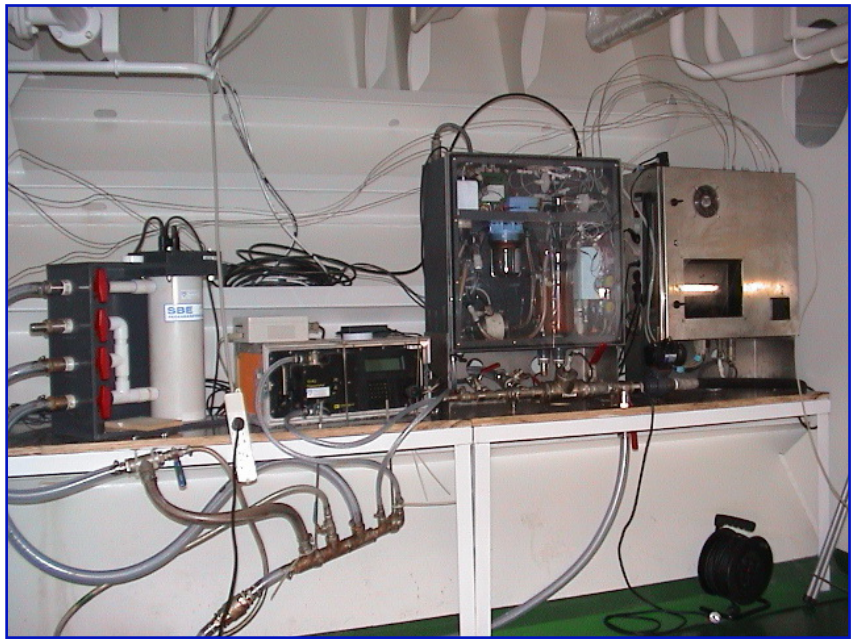

pCO_2 in the atm and sw

CO2 Studies

Time series studies

Temporal variability in a fix point

OceanicTime Series Station

Spatial and Temporal variability in a transect

VOS line

Regional studies

Oceanographic cruises

Time series studies

Temporal variability in a fix point

OceanicTime Series Station

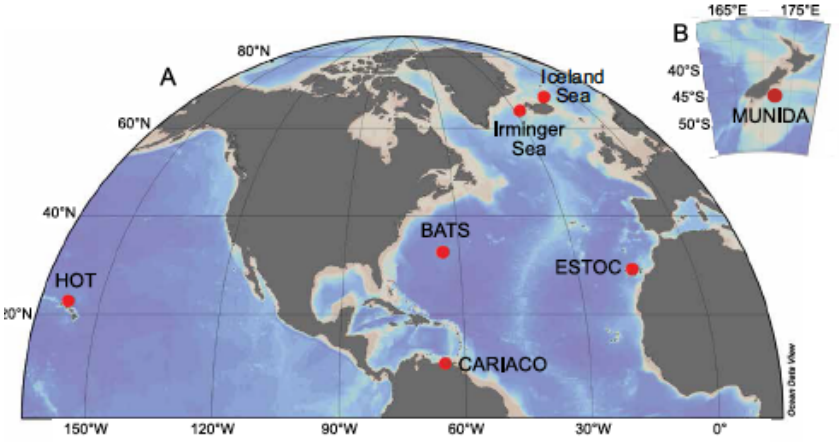

INTERNATIONAL COUNCIL OF SCIENTIFIC UNIONS
Scientific Committee on Oceanic Research

J G O F S

GLOBAL CHANGE
IGBP

Joint Global Ocean Flux Study

A Core Project of the International Geosphere-Biosphere Programme

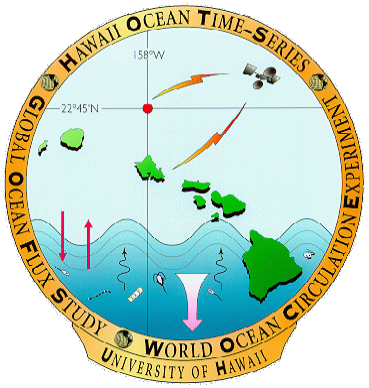

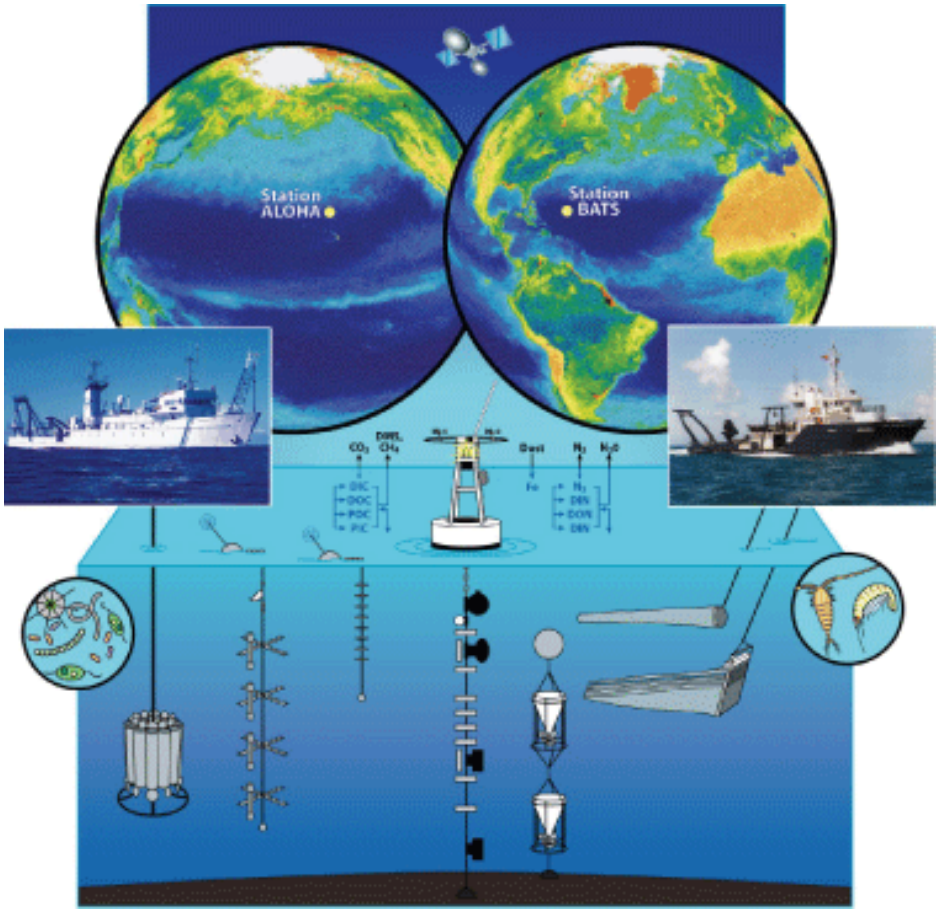

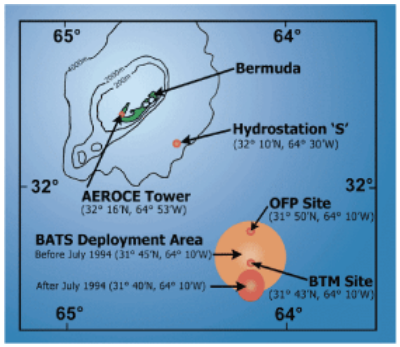

The firsts time series stations to measure the CO_2 system and biogeochemical processes in the ocean were stablished in 1989 in BATS (Bermuda) and HOT, (Hawaii) with JGOF

European Station for Time Serie in the Ocean Canary Islands

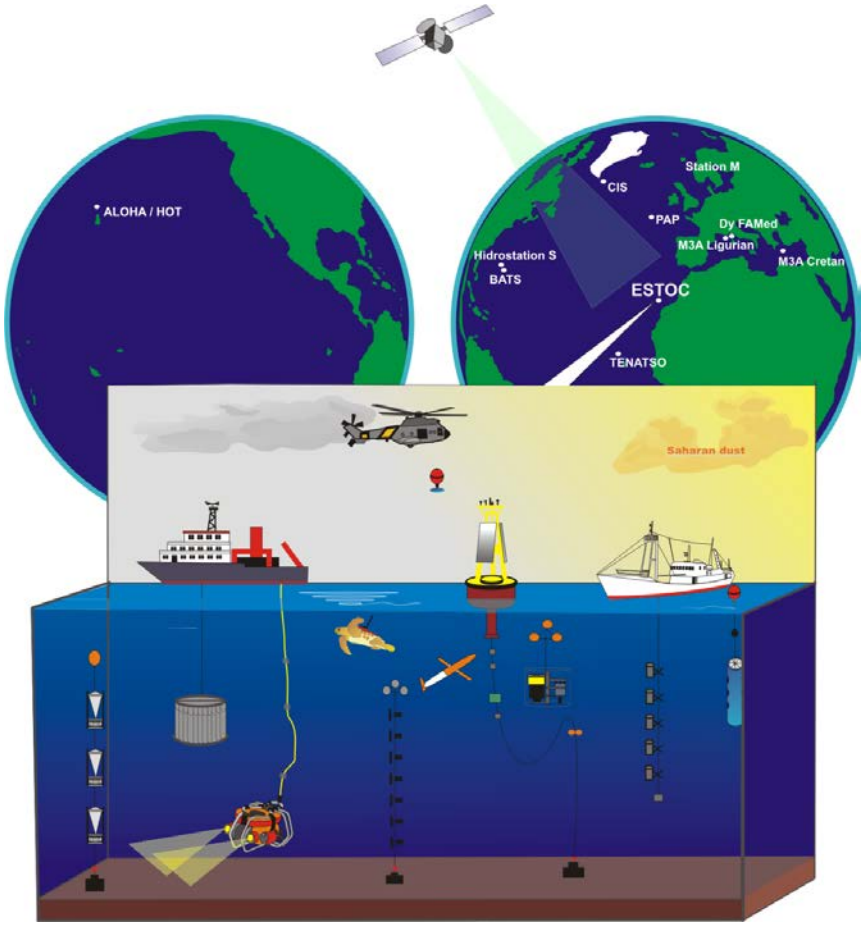

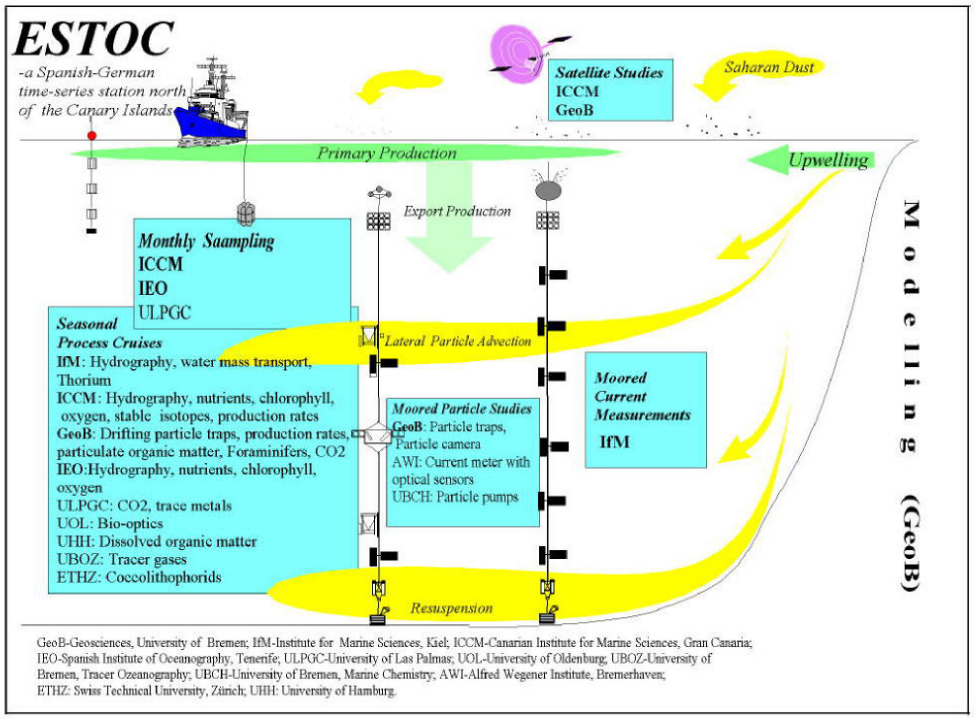

In 1994, the ESTOC station was stablished as an initiative of German program JGOF with the U. Bremen, U. Kiel, ICCM, IEO and in 1995 ULPGC was incorporated to study the CO2 system

ESTOC, Actual

ESTOC, 1994-2004 J G F S

ESTOC

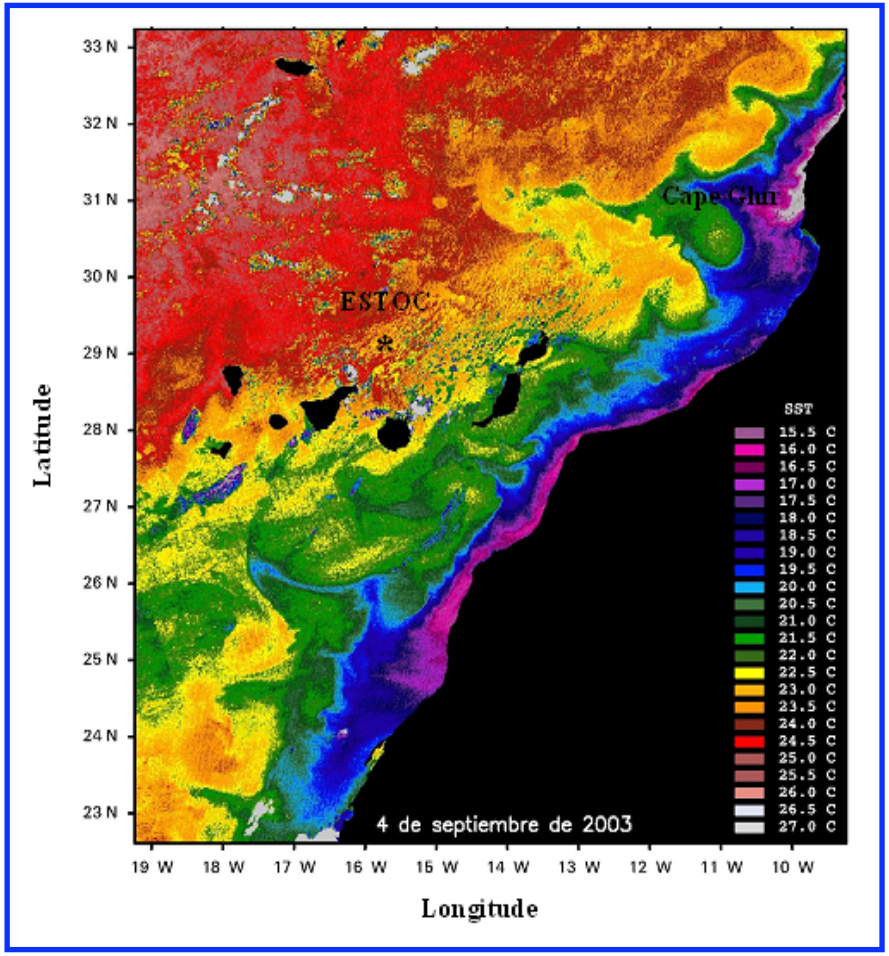

Frequency

1995-2004 (monthly)

2004-2012 (seasonal)

Actual (2-3 times/year),

2008- Buoys with sensors

Location ➔ Canary Current. Transitional zone between the North-West African coastal upwelling region and the open ocean oligotrophic waters of the North East Atlantic subtropical gyre

ESTOC – Hydrographic properties

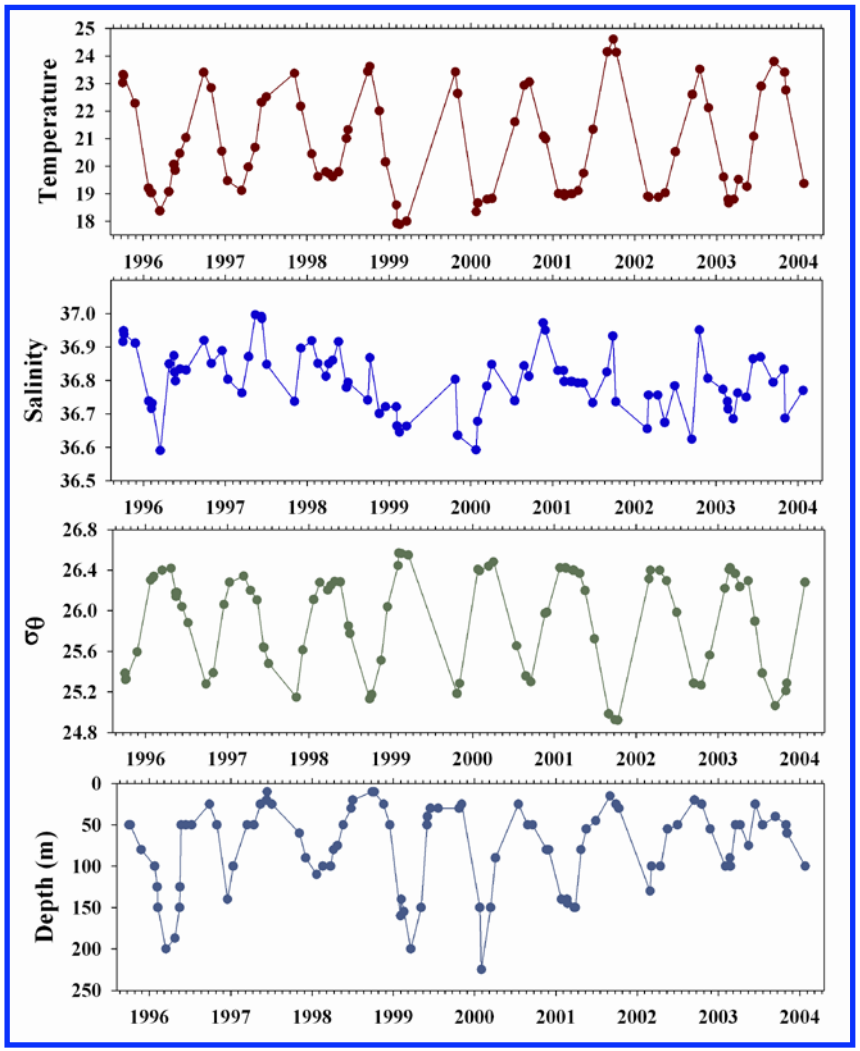

(Santana-Casiano et al., 2005)

T 18ºC -24ºC

S 36.6 -37

Density 25 to 26.4

MLD 25 -200 m

The convective mixing during winter and the stratification of the water column from May to October control the seasonal change

Fluxes of CO_2 in ESTOC site

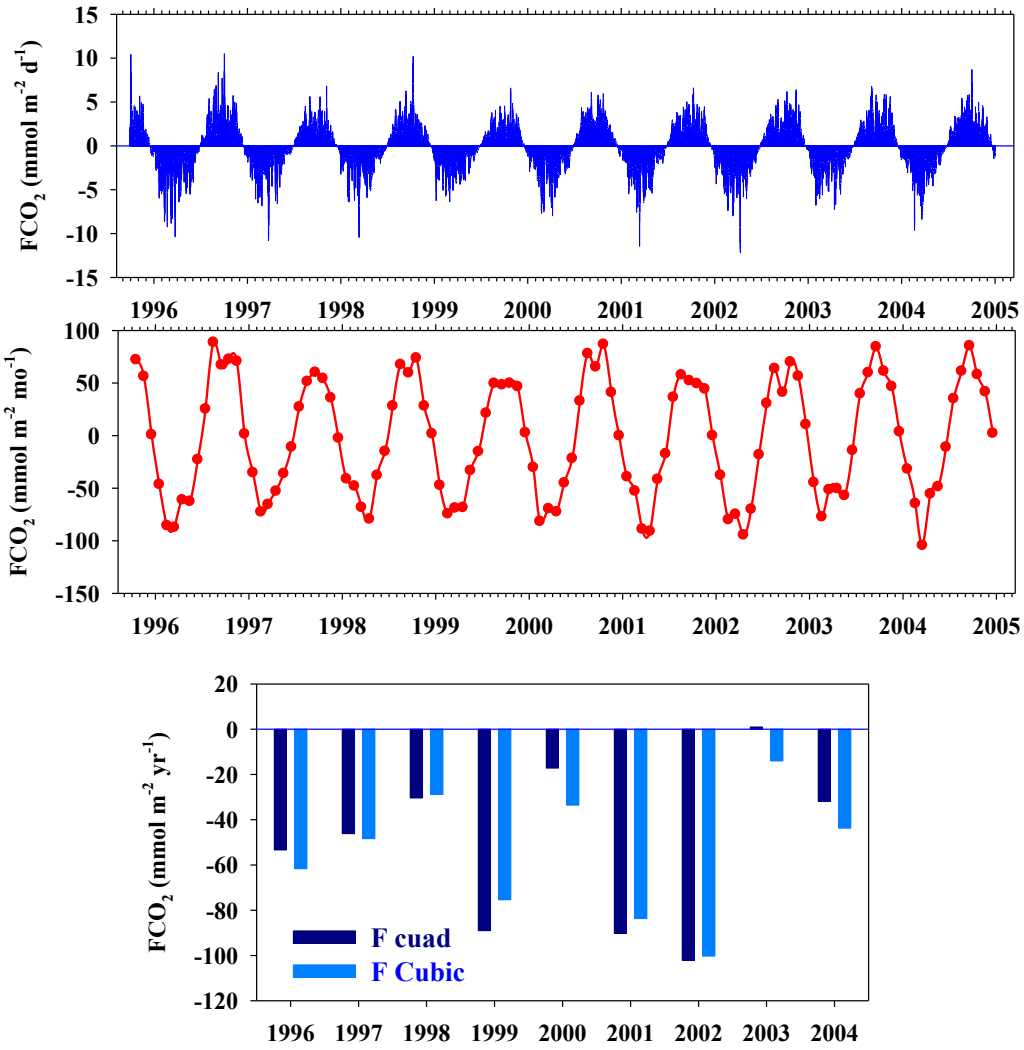

SOURCE June-November

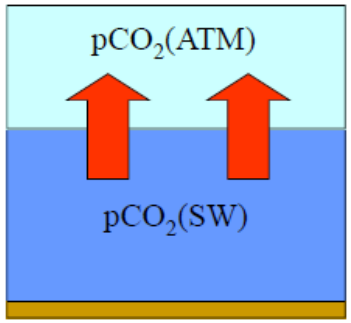

SINK December-May

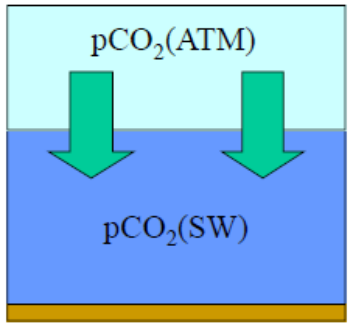

$FCO_2 = -51 \pm 36$ mmol m^{-2} yr^{-1}

(Santana-Casiano et al. 2007)

ESTOC – pH and pCO_2

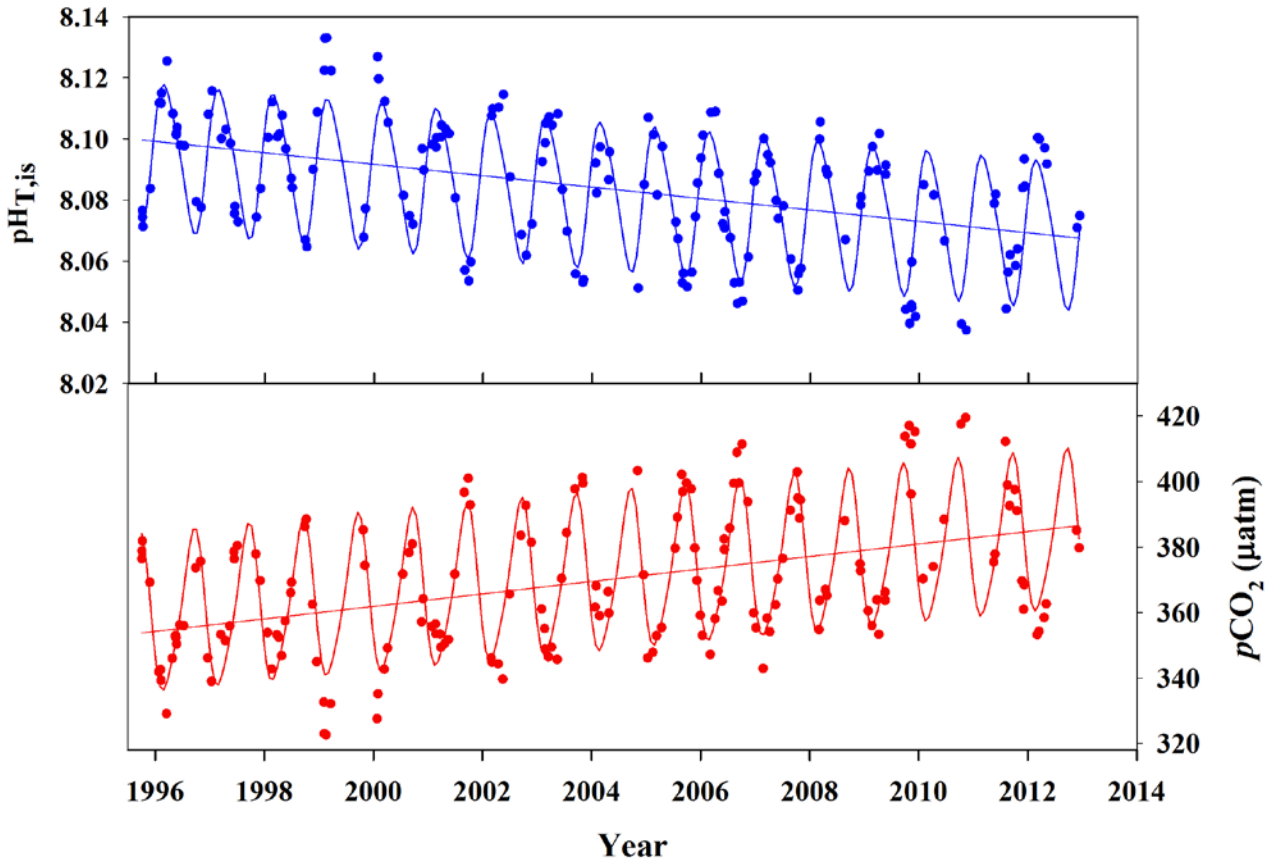

Seasonal variability

$pH_{T,is}$ 0.03-0.05

pCO_2 60-70 µatm

minimum values (320-340 µatm) in winter and maximum values (390-410 µatm) in summer.

Annual trends

$pH_{T,is}$ - 0.0019 ± 0.0003 pH units yr^{-1}

pCO_2 of 1.9±0.3 µatm yr^{-1}

ESTOC – NC_T and NA_T

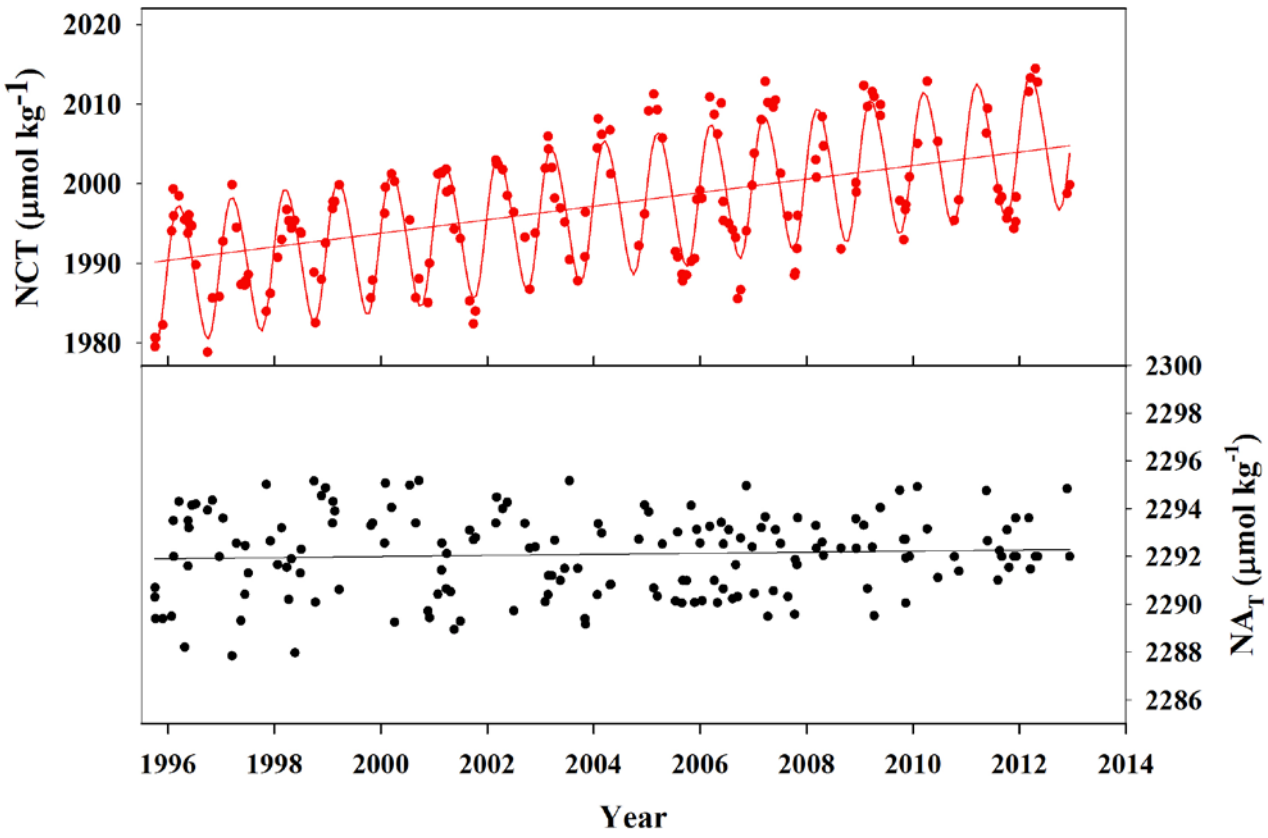

(C_T and A_T, normalized to a contant salinity of 35)

NC_T has increased by 0.9 ± 0.1 µmol kg^{-1} yr^{-1} linked to the pCO_2 increase

NA_T remains constant with a value of 2292 ± 2 µmol kg^{-1}

Introducir NAT y CT

ESTOC

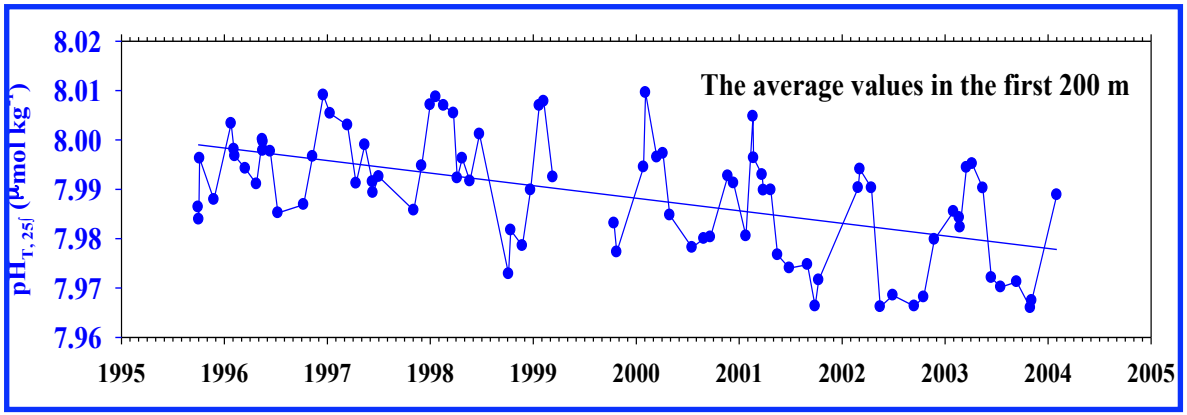

The pH decreases at a rate of 0.0012 ± 0.0004 pH units yr^{-1}

The change in pH is observed in the first 200 m but also throughout the entire water column

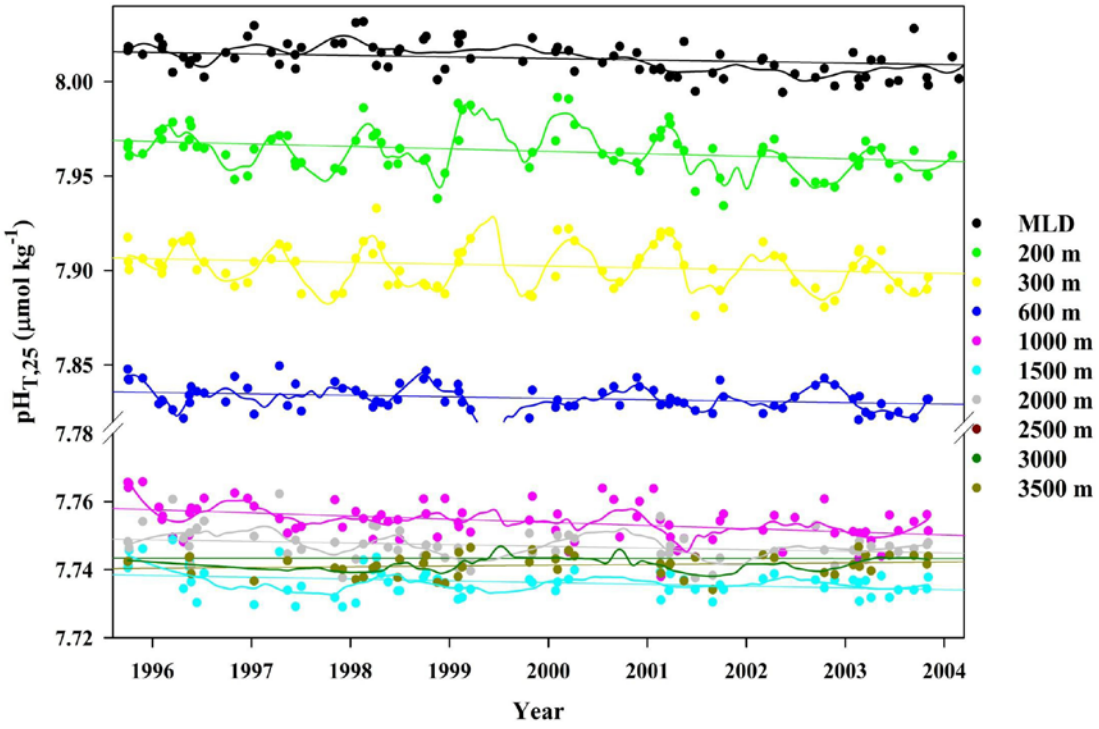

González-Dávila et al., 2010

European Time Series Stations

Integration and enhancement of key existing European deep-ocean observatories (EuroSITES). VII Programa Marco de la Unión Europea ENV.2007.4.1.3.2. Grupo 13 (2008-2010)

EuroSITES is part of the international OceanSITES network

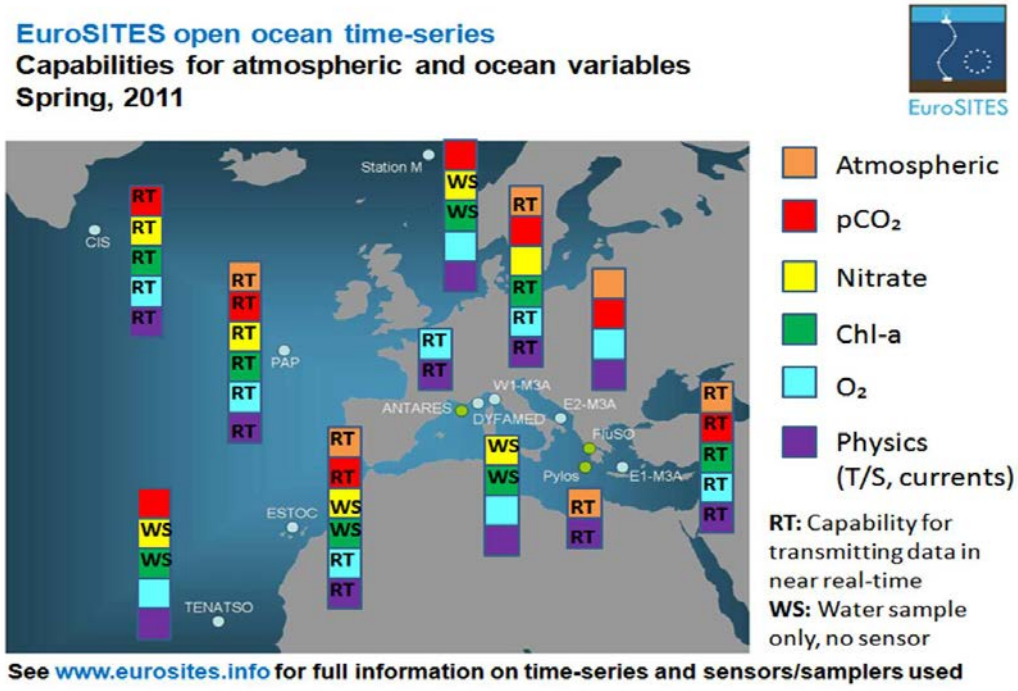

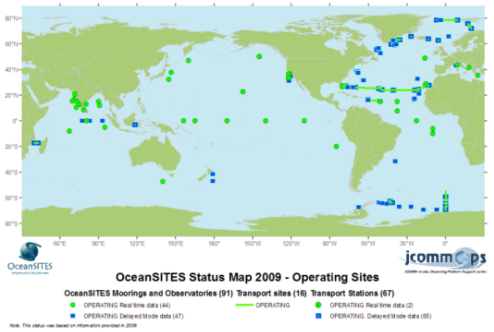

OceanSITES

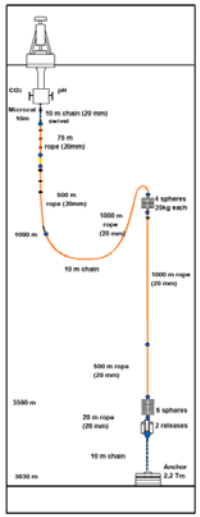

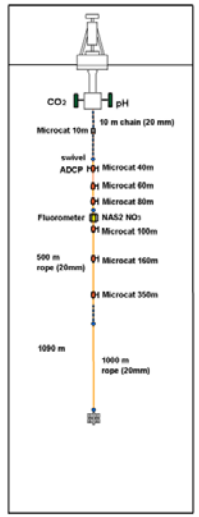

In 2008, participation in the European project EUROSITES and the ICCM (now PLOCAN) installed a buoy con T and S sensors and QUIMA included the pCO2 and pH sensors.

Oceanic CO_2 time series stations

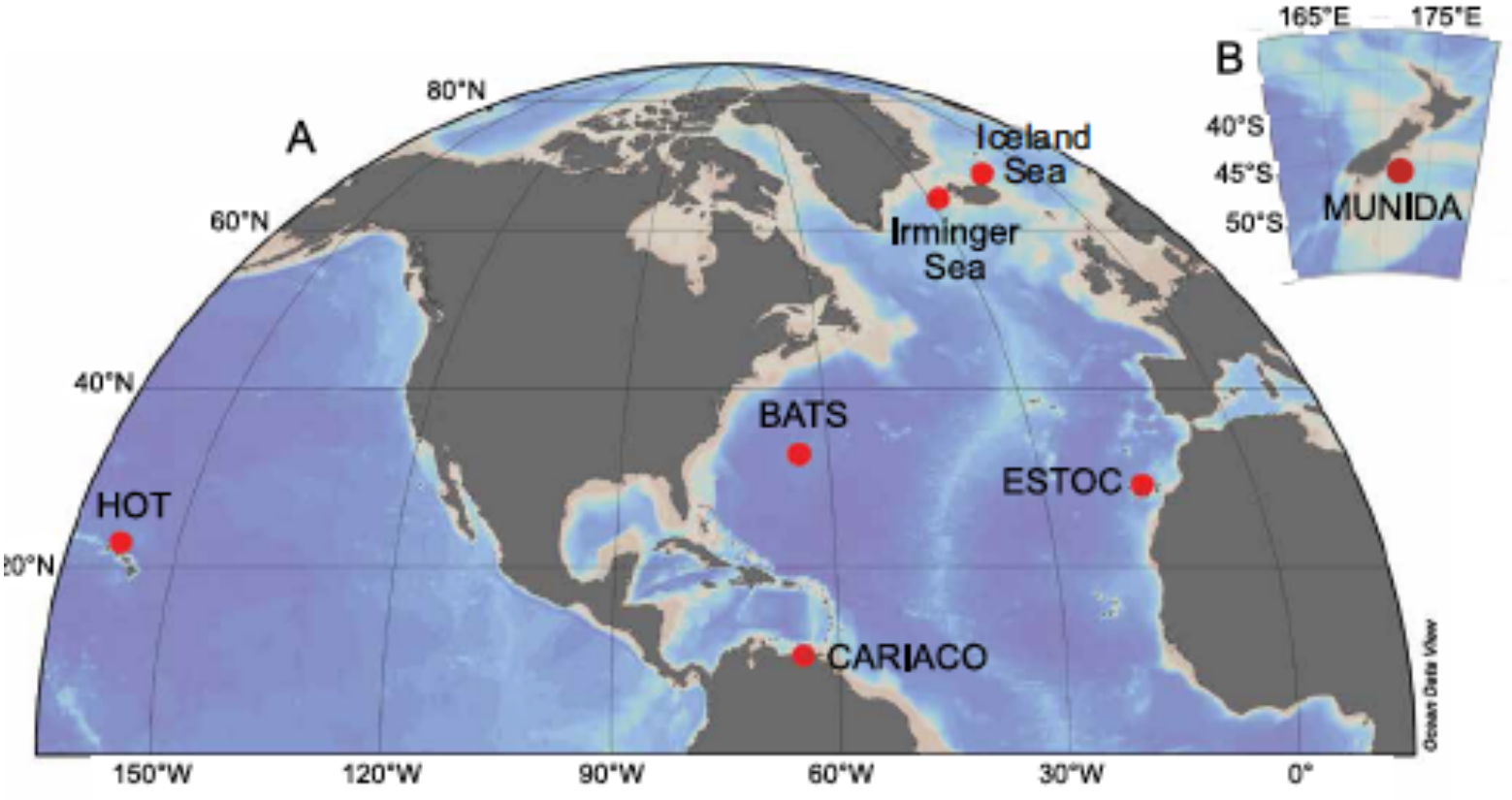

ESTOC forms part of a network of oceanic CO_2 time series stations

Bates et al., 2014

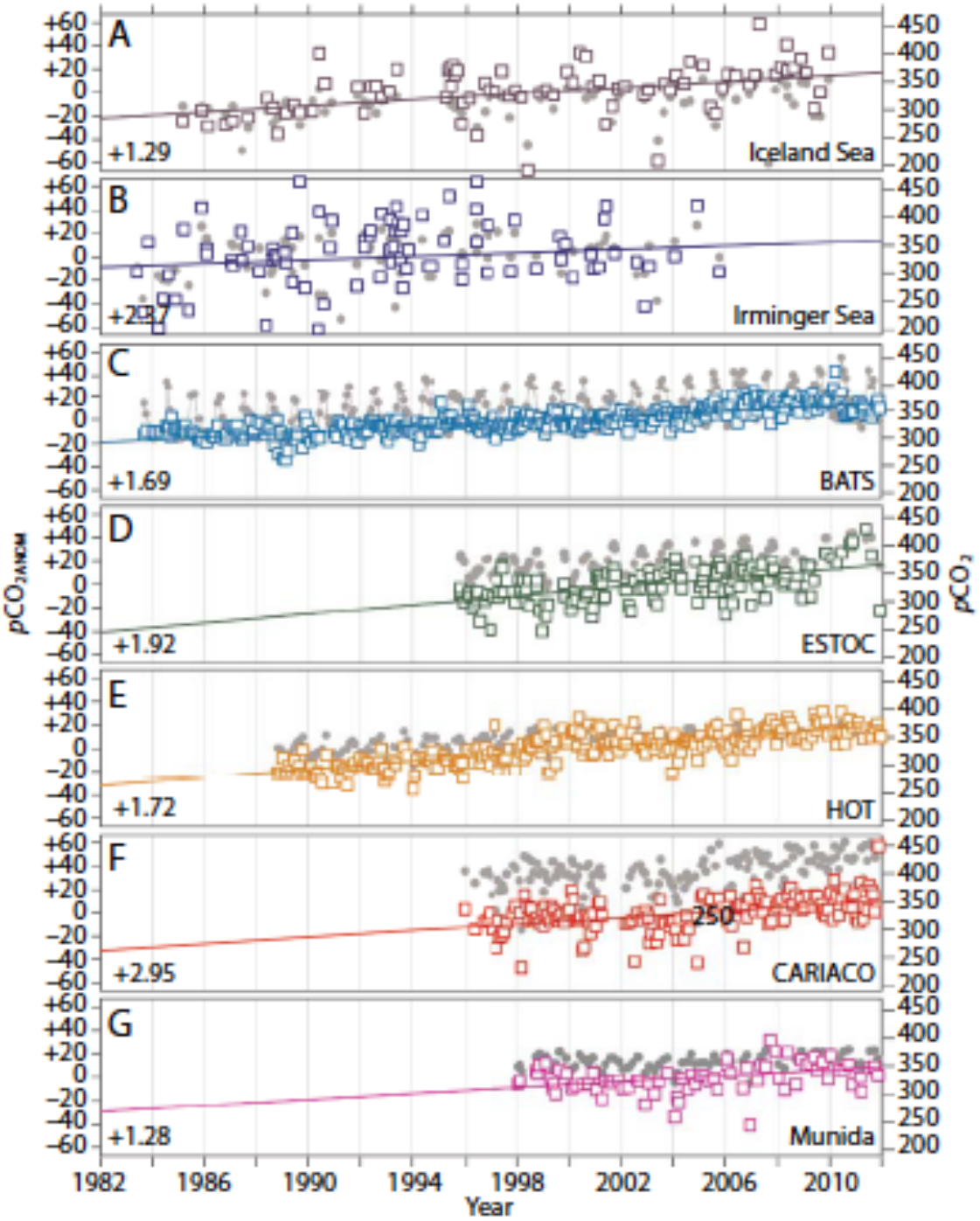

Increase in the ocean pCO_2

The trends are similar in all stations with the exception of:

Irminger Sea

The most changing, where the beginning of the THC and sink of the water take place 2.37

Cariaco

It has special characteristics for being in an upwelling region in the Caribbean 2.95

Bates et al., 2014

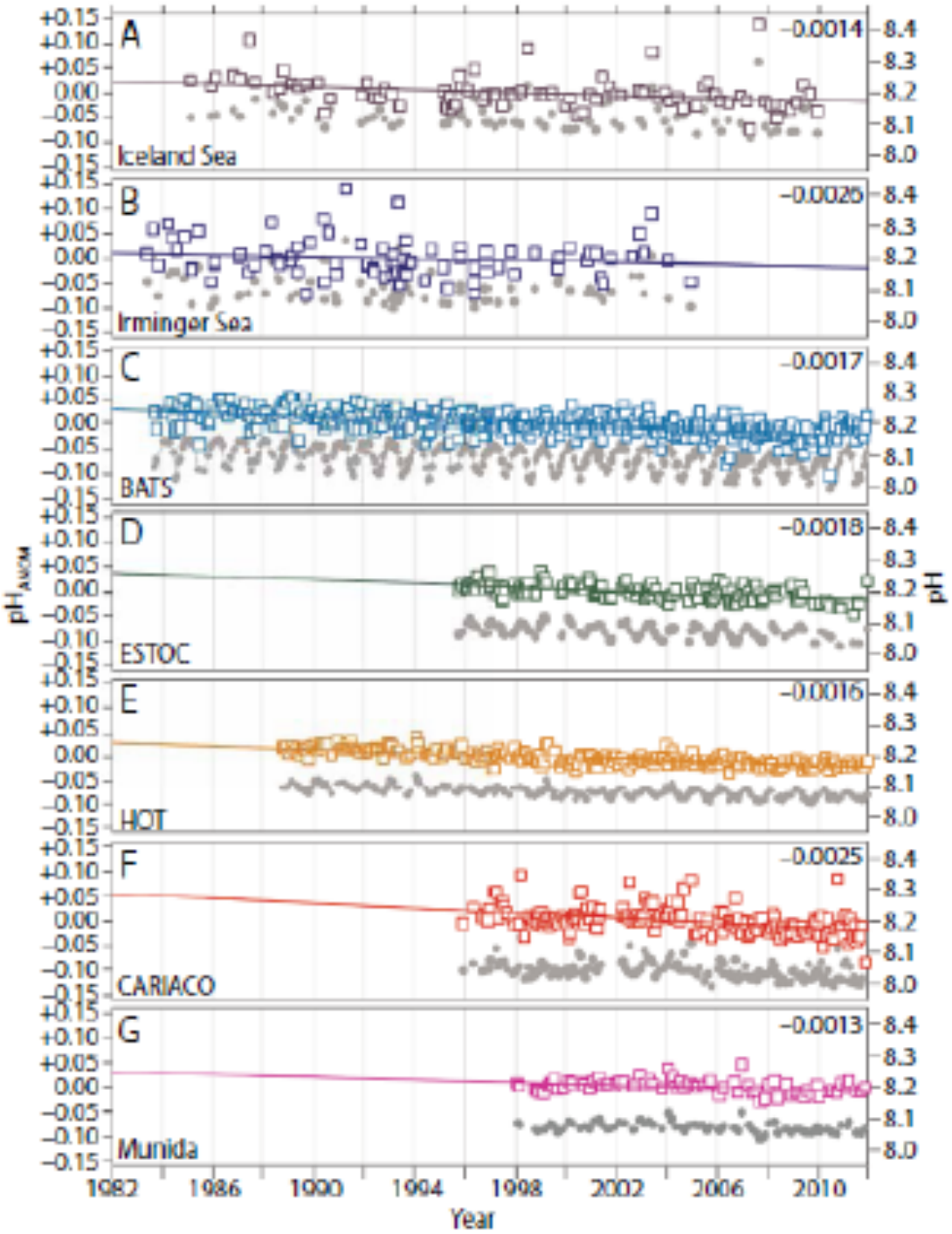

Reduction in the pH

pH has decreased in 0.1 after 1780

- 30% increase in acidity

- 16% reduction in $[CO_3^{2-}]$

Bates et al., 2014

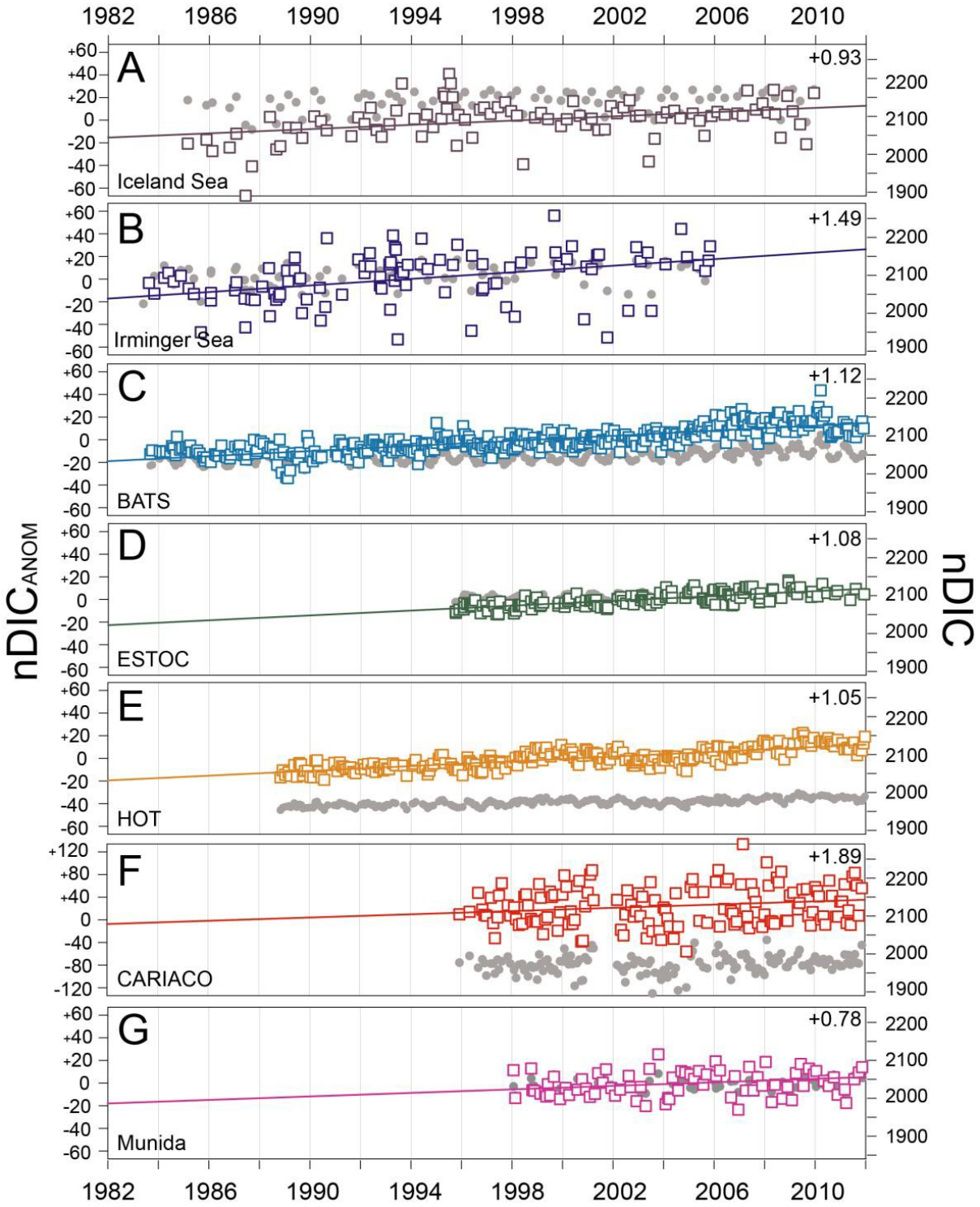

Increase in C_T (DIC)

DIC values increasing between +0.61 and +1.78 µmol kg^{-1} yr^{-1}

nDIC increased in the range +0.78 a +1.89 µmol kg^{-1} yr^{-1}

Bates et al., 2014

The data of HOT, BATS and ESTOC

WMO INTERGOVERNMENTAL PANEL ON CLIMATE CHANGE UNEP

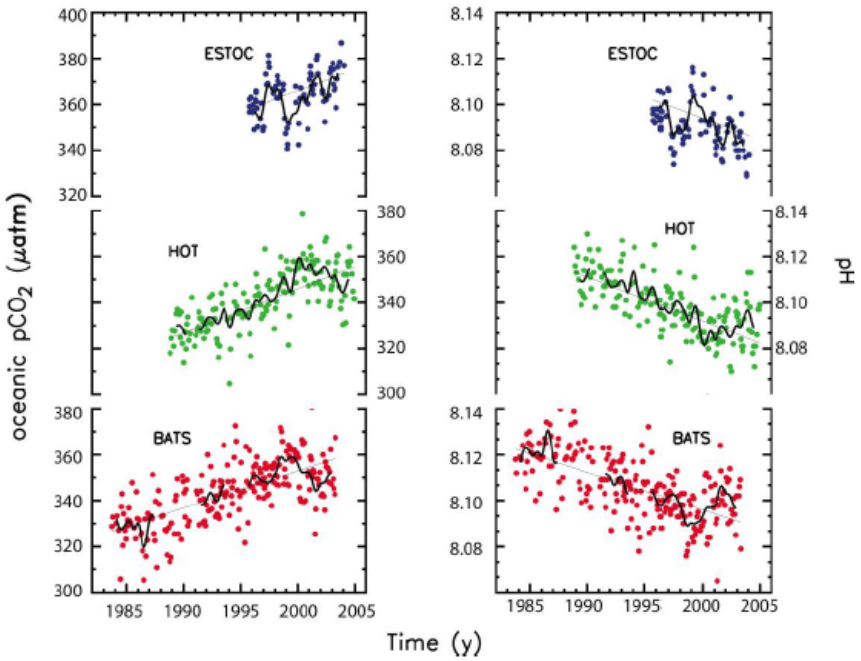

Figure 5.4.1. Changes in surface oceanic pCO_2 (left; in µatm) and pH (right) from the time-series stations at ESTOC (29°N, 15°W; (Gonzalez-Dávila et al., 2003)), HOT (23°N, 158°W; (Dore et al., 2003)) and BATS/Station S (31/32°N, 64°W; (Bates et al., 2002; Gruber et al., 2002)). pCO_2 and pH are directly measured at ESTOC and calculated from Dissolved Inorganic Carbon and alkalinity at HOT and BATS. The mean seasonal cycle was removed from all data. The thick black line filters variability less than 5 years. The thin black line is a linear fit to the data, and give an increase in pCO_2 of 1.9, 1.9, and 1.6 µatm/yr and a decrease in pH of 0.0018, 0.0019, and 0.0016 for ESTOC, HOT, and BATS respectively.

Contribution IV and V IPCC informs

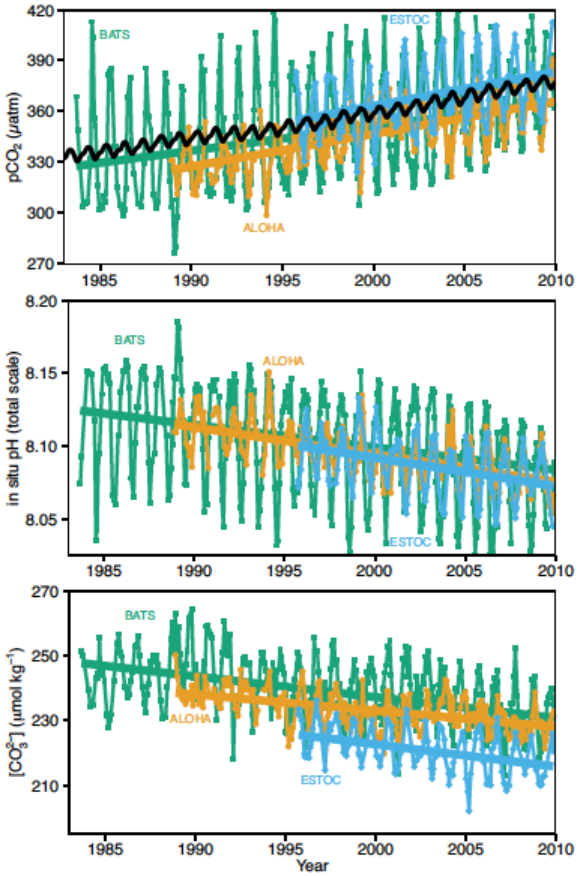

Figure 3.18 | Long-term trends of surface seawater pCO_2 (top), pH (middle) and carbonate ion (bottom) concentration at three subtropical ocean time series in the North Atlantic and North Pacific Oceans, including (a) Bermuda Atlantic Time-series Study (BATS, 31°40'N, 64°10'W; green) and Hydrostation S (32°10', 64°30'W) from 1983 to present (updated from Bates, 2007); (b) Hawaii Ocean Time-series (HOT) at Station ALOHA (A Long-term Oligotrophic Habitat Assessment; 22°45'N, 158°00'W; orange) from 1988 to present (updated from Dore et al., 2009) and (c) European Station for Time series in the Ocean (ESTOC, 29°10'N, 15°30'W; blue) from 1994 to present (updated from González-Dávila et al., 2010). Atmospheric pCO_2 (black) from the Mauna Loa Observatory Hawaii is shown in the top panel. Lines show linear fits to the data, whereas Table 3.2 give results for harmonic fits to the data (updated from Orr, 2011).

Emphasize the effect that anthropogenic carbon has on the increase of pCO_2 in the ocean and its acidification

http://www.climatechange2013.org/images/report/WG1AR5_Chapter03_FINAL.pdf

CO2 Studies

Time series studies

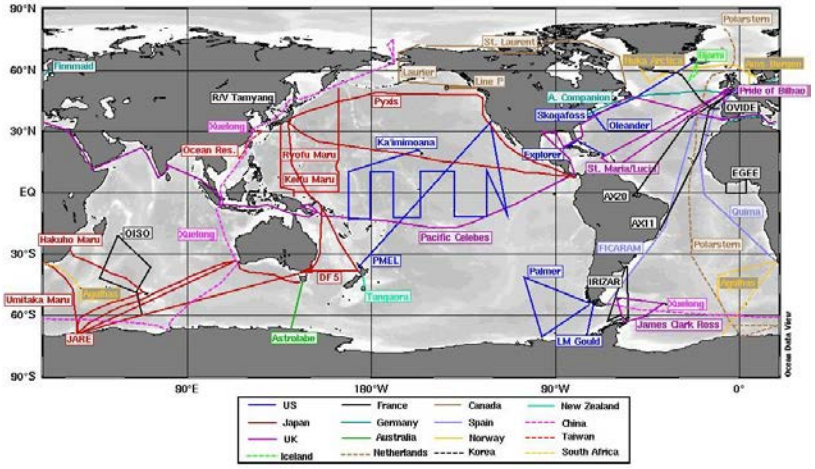

Spatial and Temporal variability

VOS line

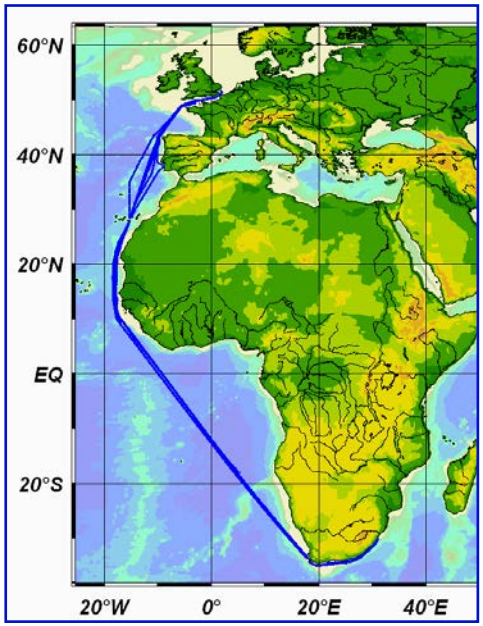

QUIMA VOS-line: UK-Cape Town-Durban

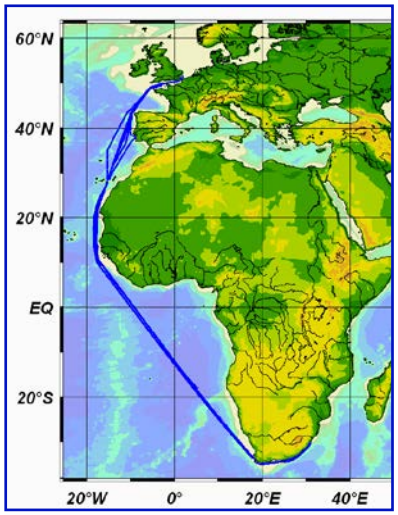

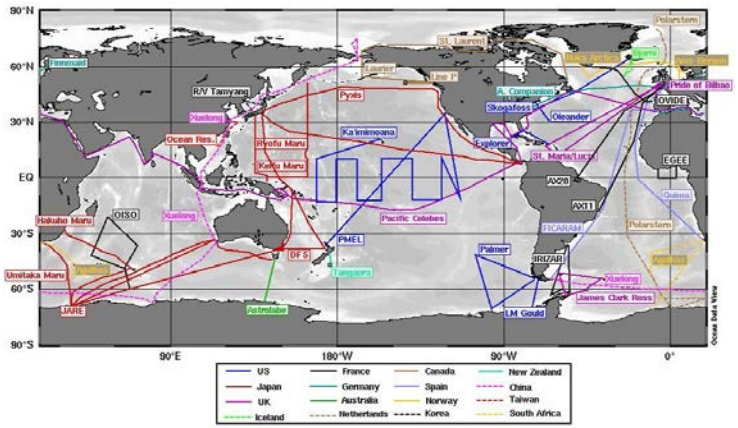

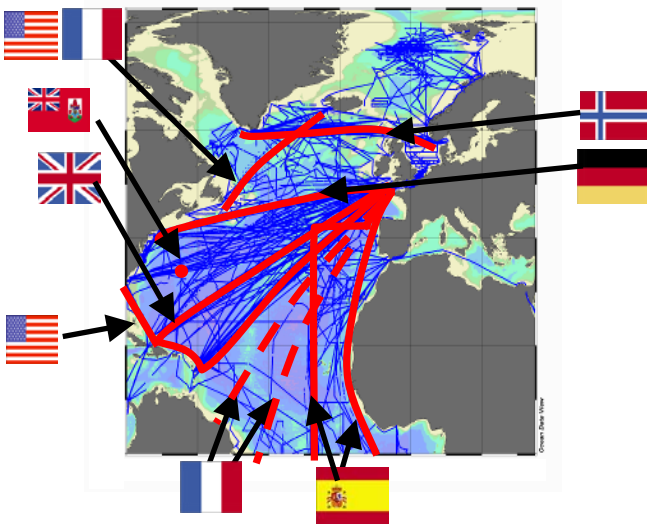

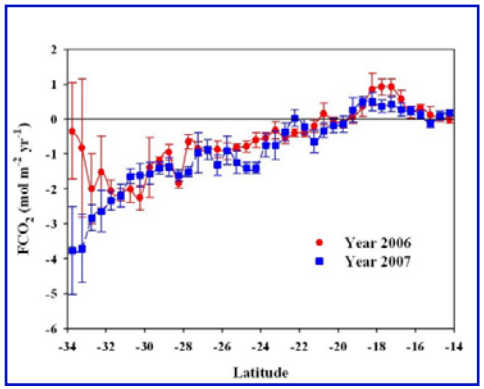

Proyectos europeos

CARBOOCEAN
2005-2009

CARBOCHANGE
2011-2015

AtlantOS
H2020
2017-2020

Tracking the Variable North Atlantic Sink for Atmospheric CO_2

Andrew J. Watson,[1*] Ute Schuster,[1] Dorothee C. E. Bakker,[1] Nicholas R. Bates,[2] Antoine Corbière,[3] Melchor González-Dávila,[4] Tobias Friedrich,[5] Judith Hauck,[1†] Christoph Heinze,[6] Truls Johannessen,[6] Arne Körtzinger,[5] Nicolas Metzl,[3] Jon Olafsson,[7] Are Olsen,[6,8] Andreas Oschlies,[5] X. Antonio Padin,[9] Benjamin Pfeil,[6] J. Magdalena Santana-Casiano,[4] Tobias Steinhoff,[5] Maciej Telszewski,[1] Aida F. Rios,[9] Douglas W. R. Wallace,[5] Rik Wanninkhof[10]

Science 326, 1391-1393 (2009)

QUIMA VOS-line: Mauritanian upwelling

2005-2012

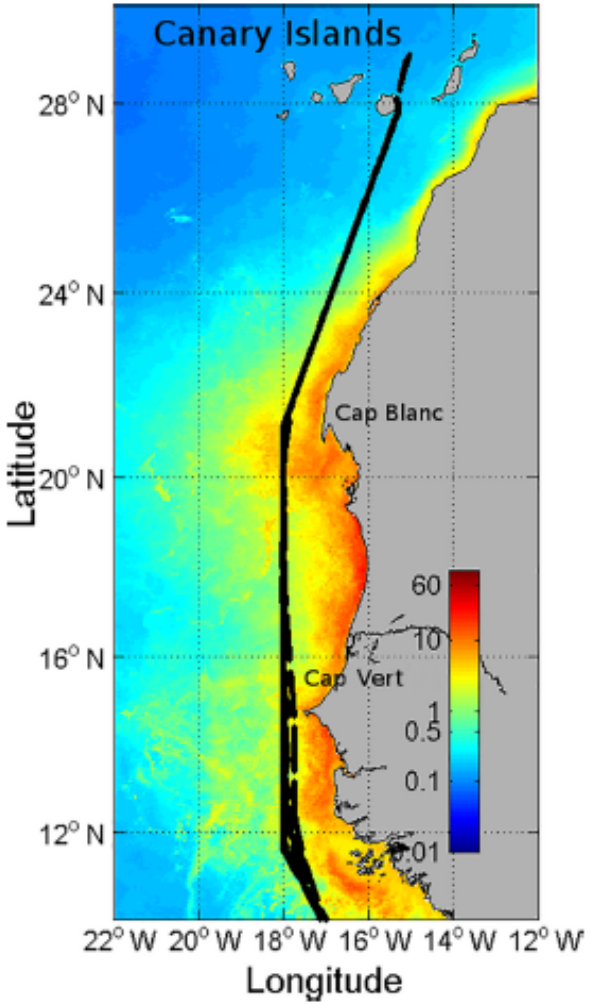

(González-Dávila et al., 2017)

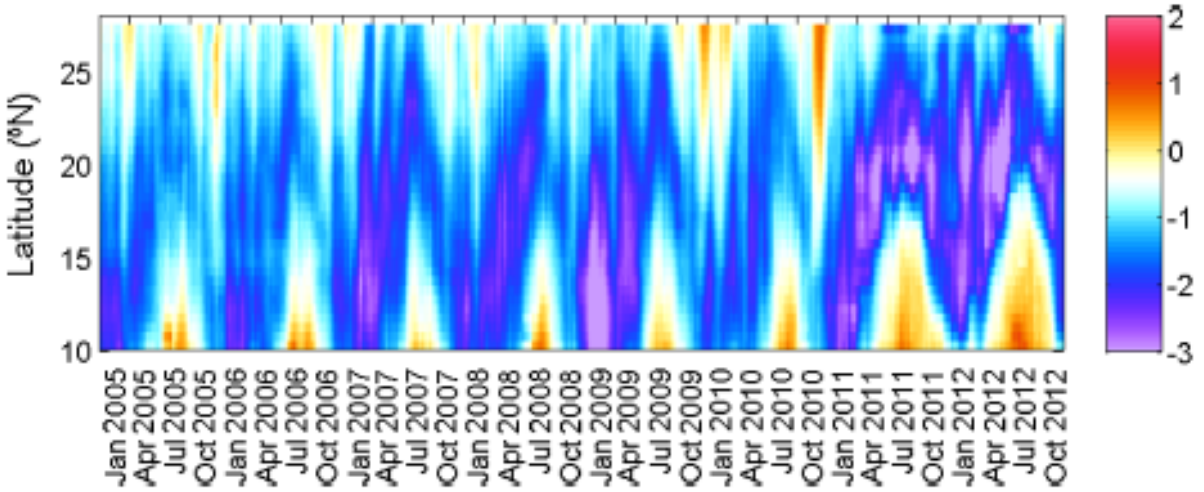

Figure 2. Time series of upwelling index (UI, $\times 10^{-3}$ m^2 s^{-1}) in the Mauritanian–Cap Vert upwelling region along the ship track computed following Nykjaer and Van Camp (1994). Blue colors are related to upwelling events and red colors to downwelling events.

North of 20ºN, upwelling conditions were favorable throughout the year, the highest upwellings were observed from March to September with a northward shift from 20º to 22ºN.

South of 20ºN, marked seasonality with favourable upwelling conditions during autumn and winter (maximum intensity January and February). Downwelling is present between May-November (summer trade winds are replaced by the monsoonal winds advecting warm water northward along the shore).

QUIMA VOS-line: Mauritanian upwelling

Latitudinal distribution of fCO_2^{sw} grouped by seasons

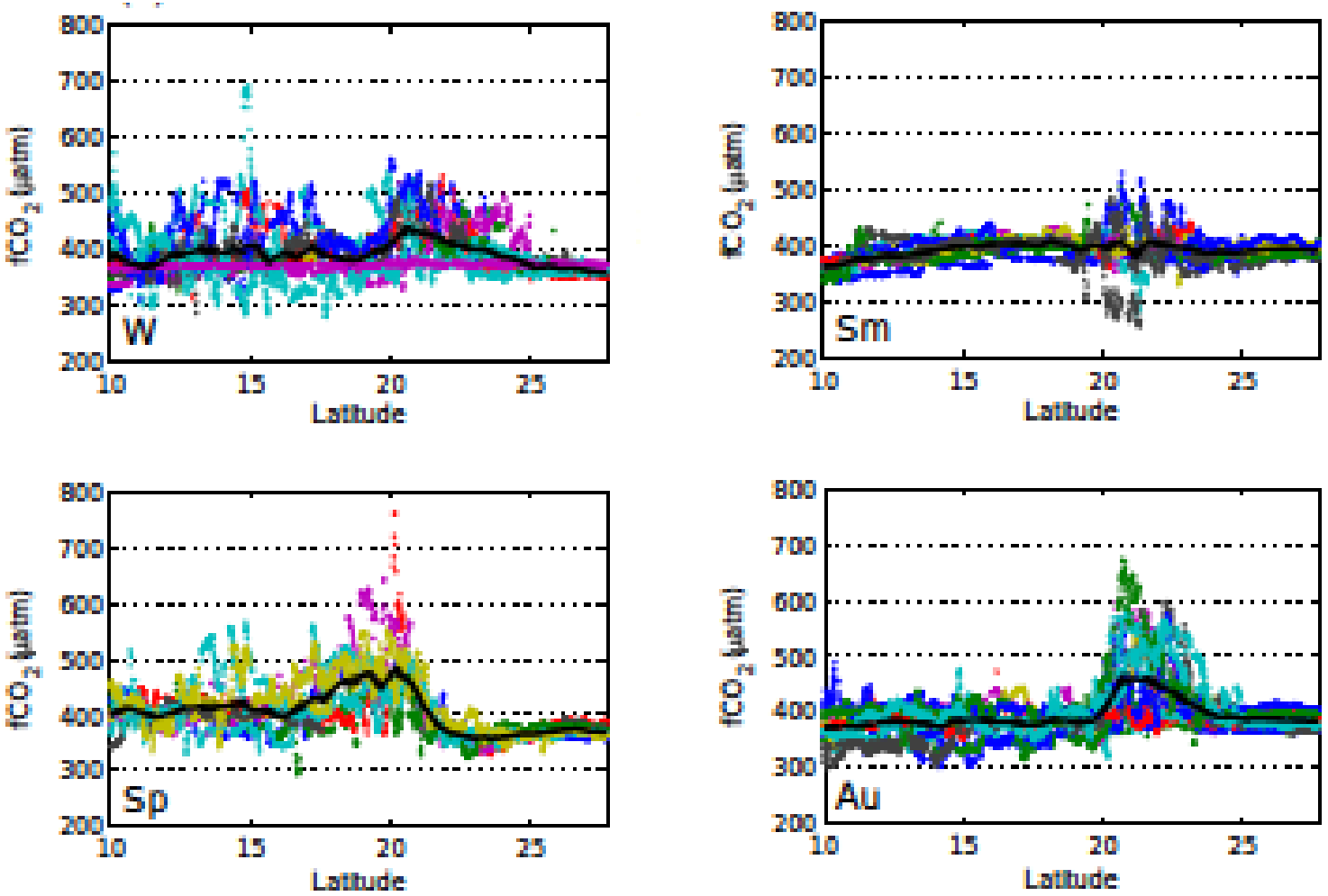

*f*CO2 ➔ spatial and temporal variability dominated by the presence of the upwelling, reaching maximum values of 750 µatm at 21ºN (Cape Blanc) during spring

(González-Dávila et al., 2017)

QUIMA VOS-line: Mauritanian upwelling

pH ➔ 21ºN (Cape Blanc)

Using the pCO_2 and the alkalinity data, the pH have been computed and the corresponding trend calculated

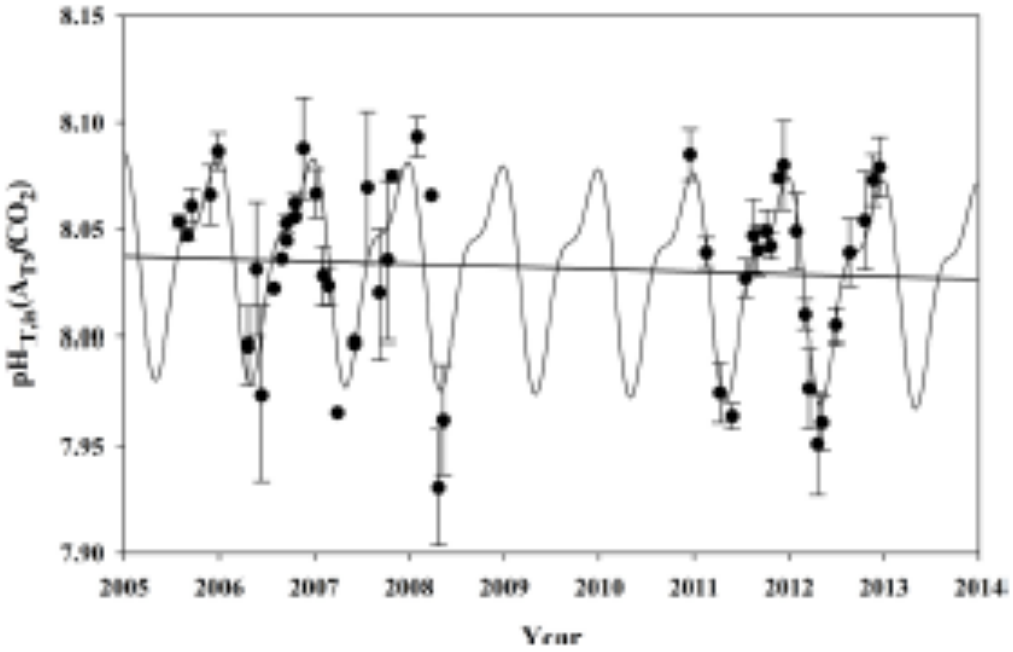

pH rate decreases at -0.003 ± 0.001 yr^{-1}

One of the highest rate values determined in CO_2 time series stations

González-Dávila et al., 2017

Fluxes of CO_2 in Mauritanian-Cape Vert

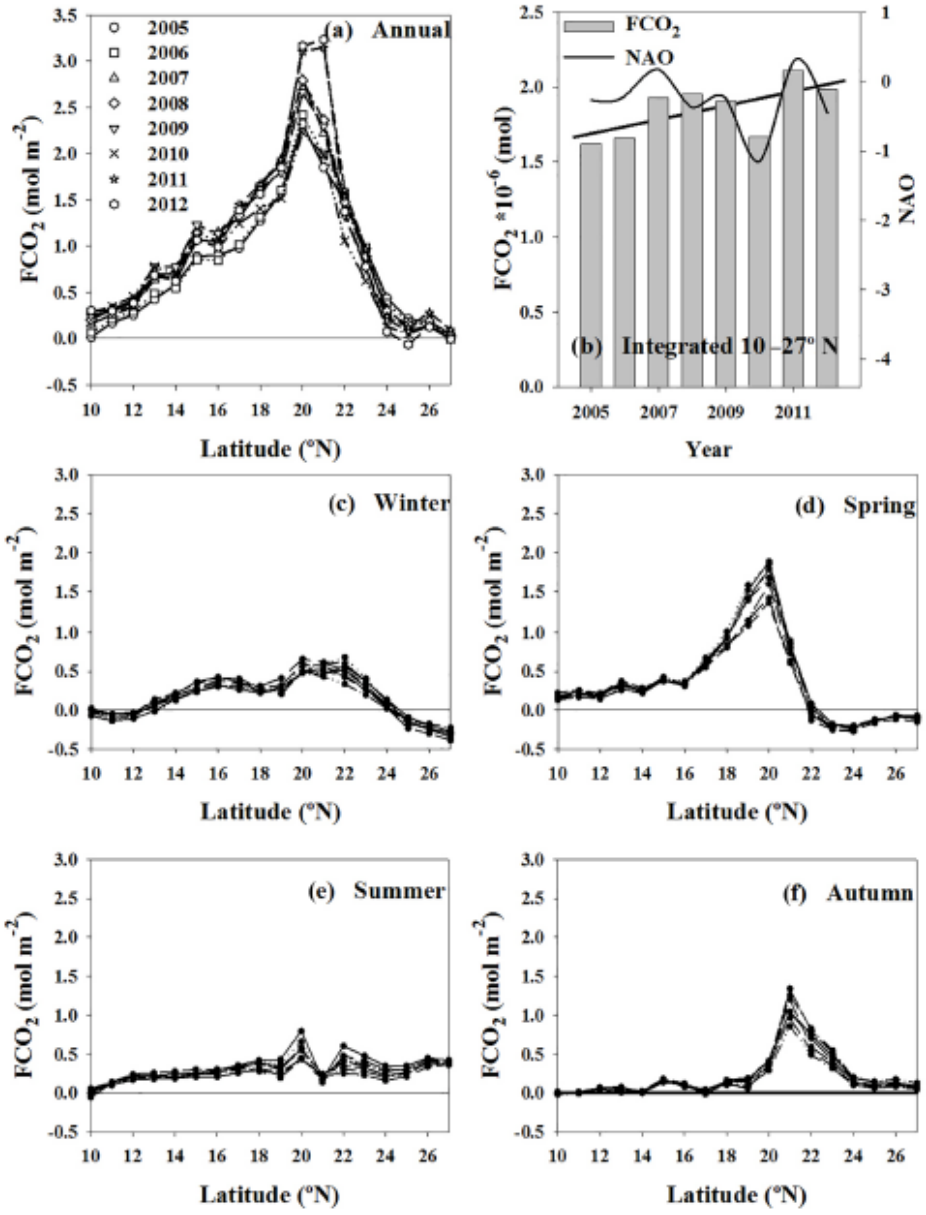

The annual FCO_2 for the full domain is positive

THE AREA IS A SOURCE OF CO_2

Cap Blanc 3.3 mol CO2 m^{-2}
North of 24◦N, $+0.14 \pm 0.03$ mol CO_2 m^{-2}
(area not affected by the coastal upwelling)

For all the area, 2005-2012
Increase of 0.6 Tg yr^{-1} in CO_2 outgassing due to increased wind speed, despite increased primary productivity.

$$FCO_2 = 0.24 \cdot k \cdot s \cdot (fCO_2^{sw} - fCO_2^{atm}),$$

$$k = (0.222 \cdot W^2 + 0.333 \cdot w) \cdot (Sc/660)^{-1/2},$$

(González-Dávila et al., 2017)

Summary

QUIMA VOS-line: CO2 Fluxes in the East Atlantic

Upwellings

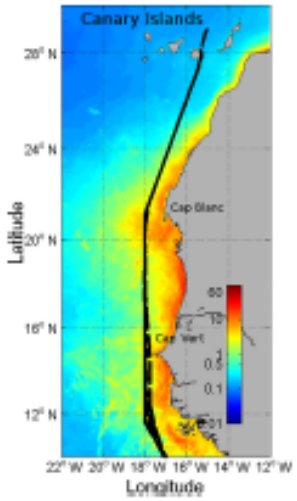

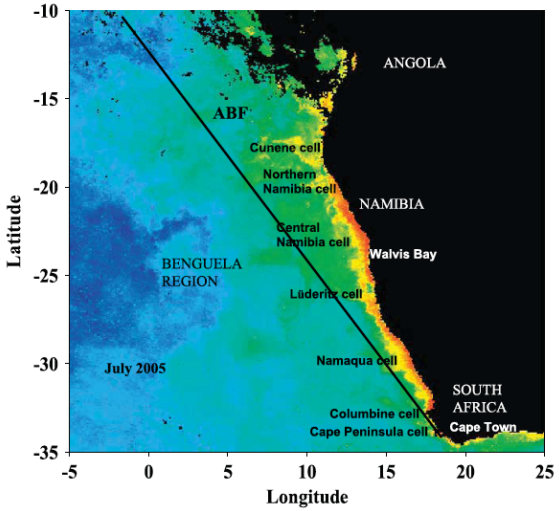

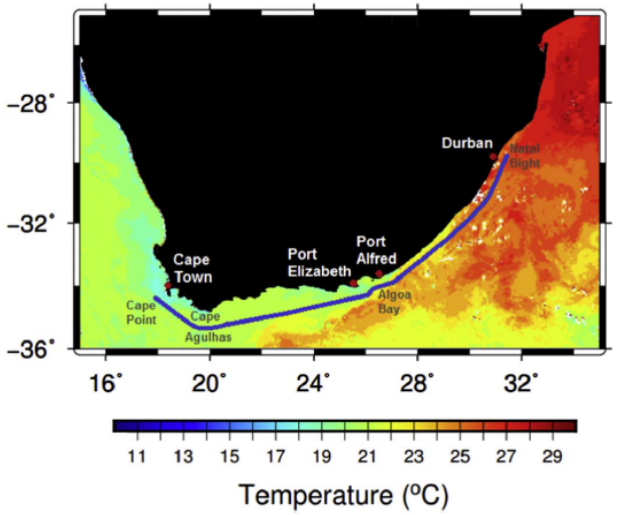

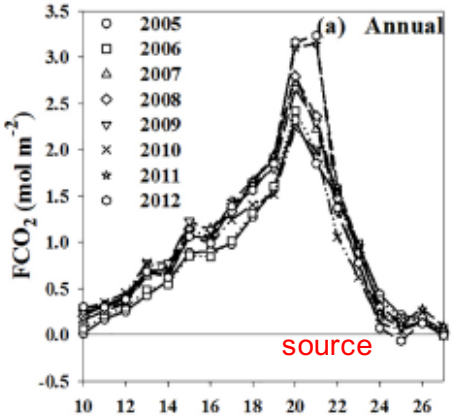

González-Dávila et al., 2017

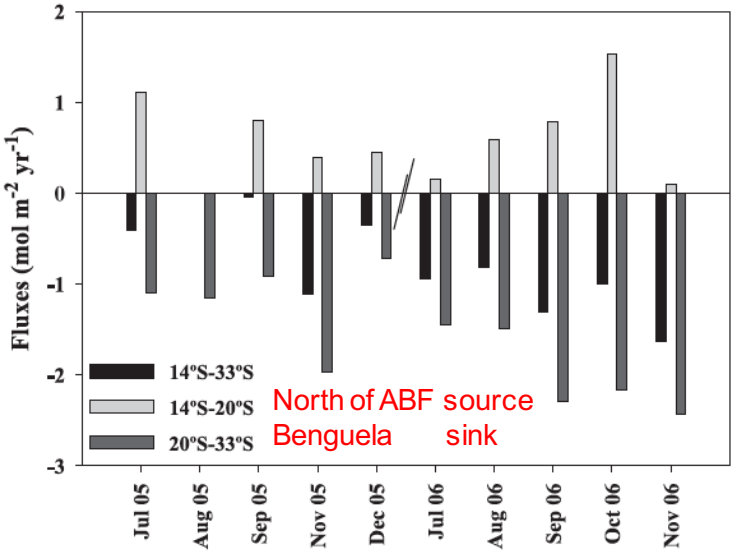

Santana-Casiano et al., 2017

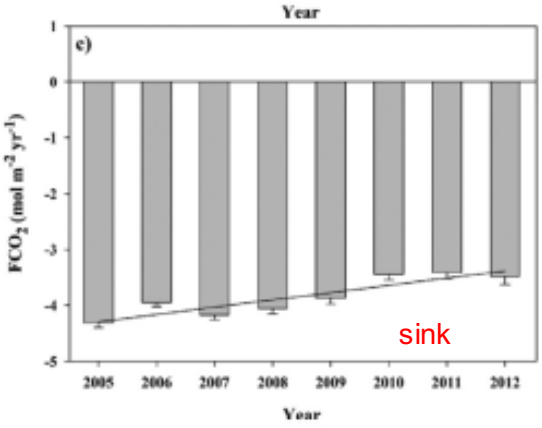

Arnone et al., 2017

CO2 Studies

Regional studies

Canary Region

Coastal studies

CANARY Region

Cruise track and stations of cruise 37/2 of R/V METEOR in January 1997

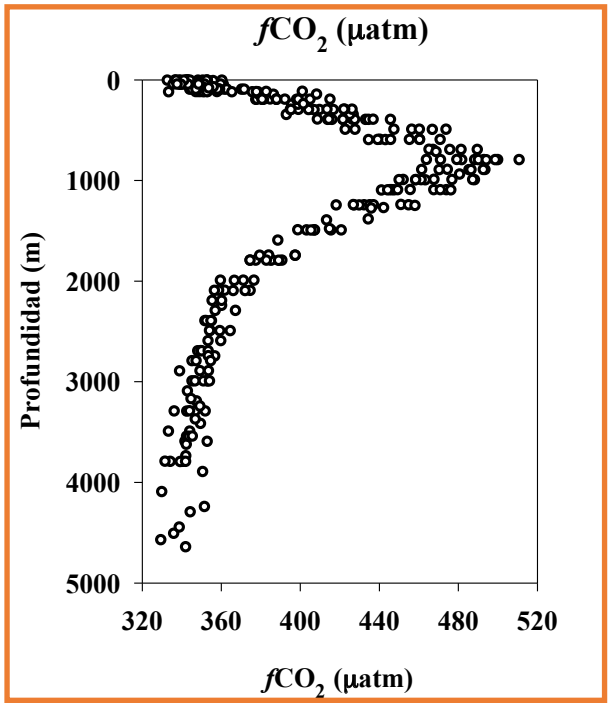

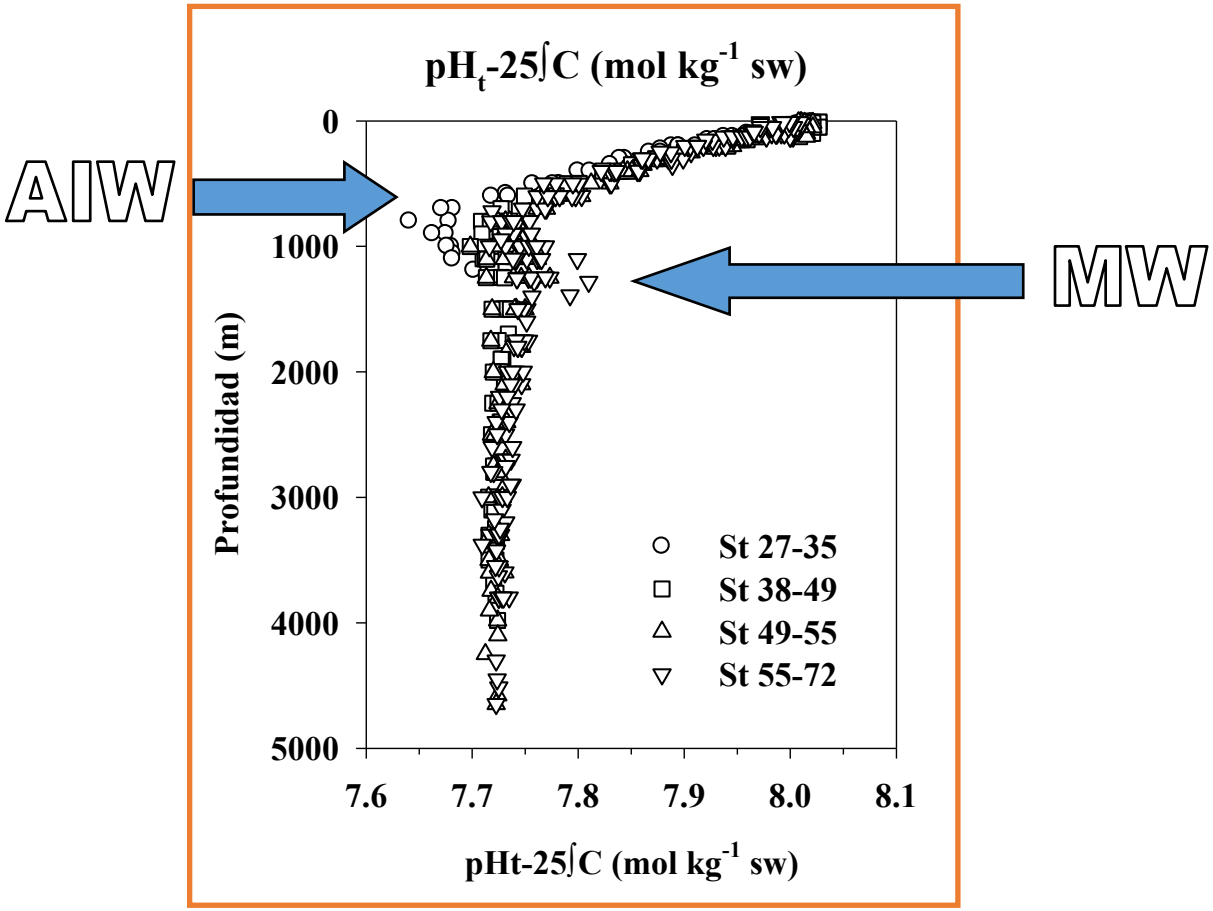

Vertical profile of fCO_2 and pH, in the Canary Islands area, Oceanographic Campaign METEOR 37 (González Dávila and Santana Casiano)

CANARY Region

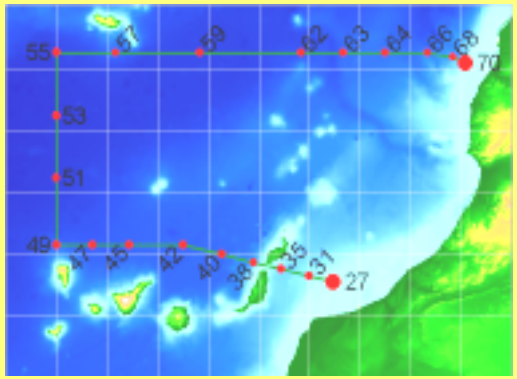

Cruise track and stations of cruise 37/2 of R/V METEOR in January 1997

$$NA_T = A_T x \frac{35}{S}$$

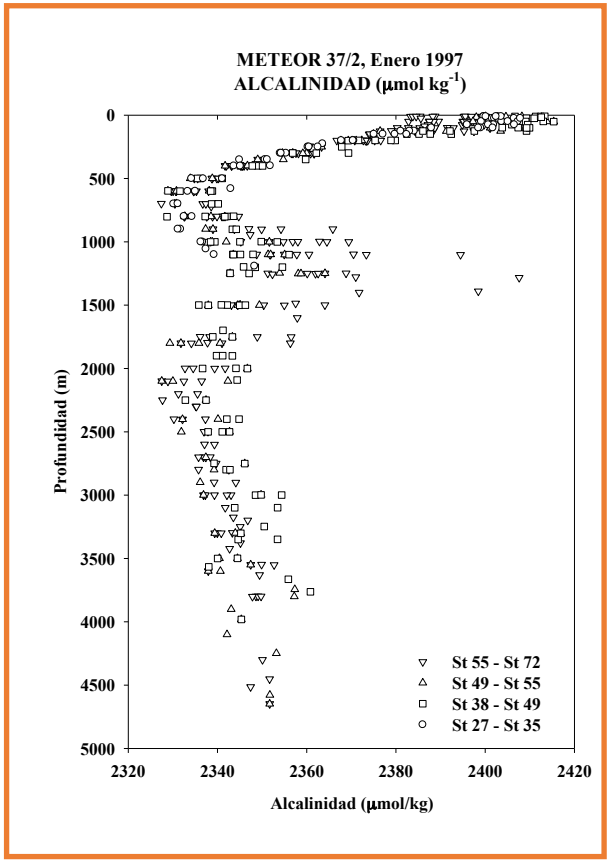

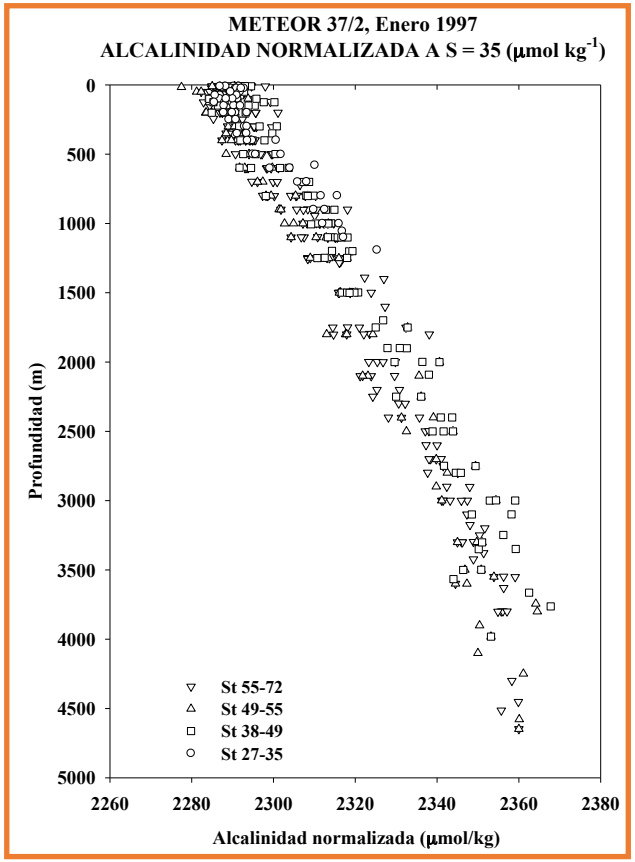

Vertical profiles of total Alkalinity and total Alkalinity normalized to a constant salinity of 35 in the Canary area, during the METEOR 37 campaign (González Dávila and Santana Casiano)

¿ ARE THE OPEN SEA TRENDS APPLICABLE TO THE COASTAL REGIONS?

CanOA- CanBio

Jan 19 – Dec- 22

Project with public-private financing

LORO PARQUE FUNDACIÓN WE CARE

Gobierno de Canarias

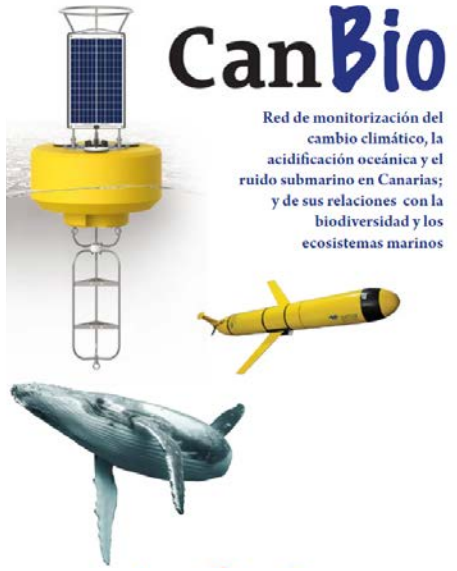

Participation of two shipping companies

FRED. OLSEN Express

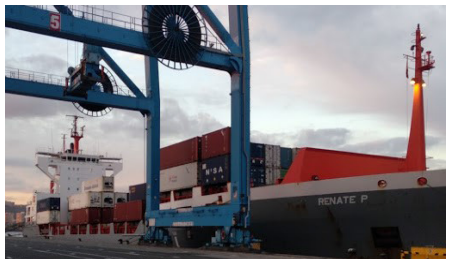

NISA MARITIMA

Changes in the CO2 system

$\uparrow fCO_2$ ➡ $\downarrow pH$ ➡ $\uparrow C_T$

$CO_2 + H_2O \rightarrow H_2CO_3 \rightarrow H^+ + HCO_3^-$

$HCO_3^- \rightarrow H^+ + CO_3^{2-}$

$H^+ + CO_3^{2-} \rightarrow HCO_3^-$

$CO_2 + CaCO_3 + H_2O \rightarrow 2\,HCO_3^- + Ca^{2+}$

Inorganic carbon and boron speciation

Buffer intensity

Revelle factor

Calcium carbonate saturation state

Other chemical reactions

Inorganic carbon and boron speciation

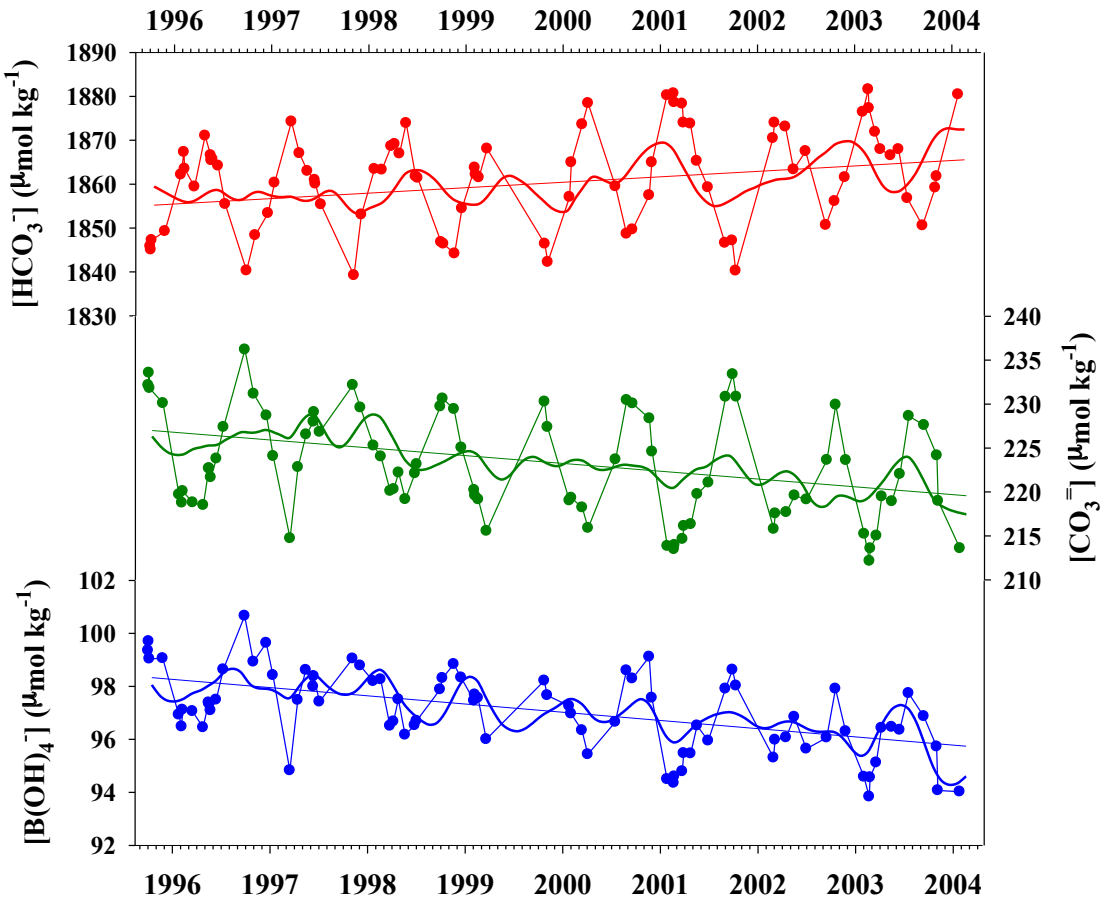

Per decade

12.4 µmol kg^{-1}

-9 µmol kg^{-1}

-3 µmol kg^{-1}

Buffer intensity

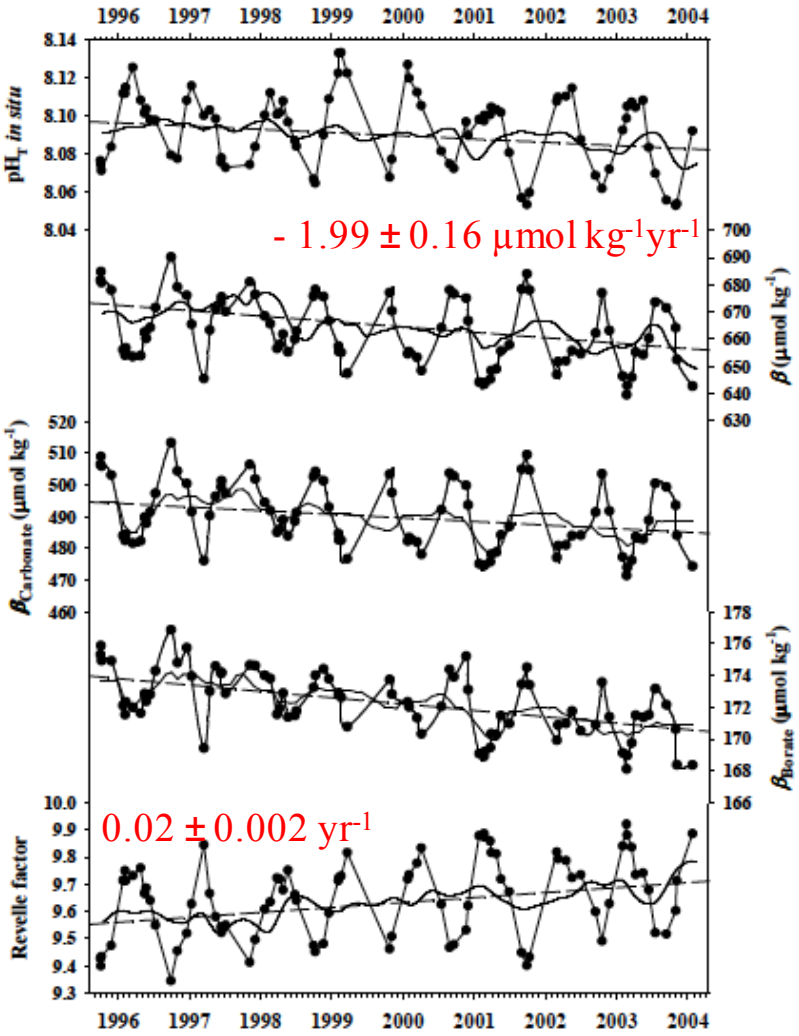

Changes in the pH affect to the acid-base equilibria of the carbonic and boric systems, the two most important buffer systems in seawater

affecting to

- the buffer capacity that decreases at a rate of 1.99
- the Revelle factor that increases at a rate of 0.02.

Buffer intensity

capacity of the solution to maintain the pH in a range

Two regions of high buffer intensity (around 1200 µmol kg-1) at the pH values corresponding with the pK* values of the carbonic acid.

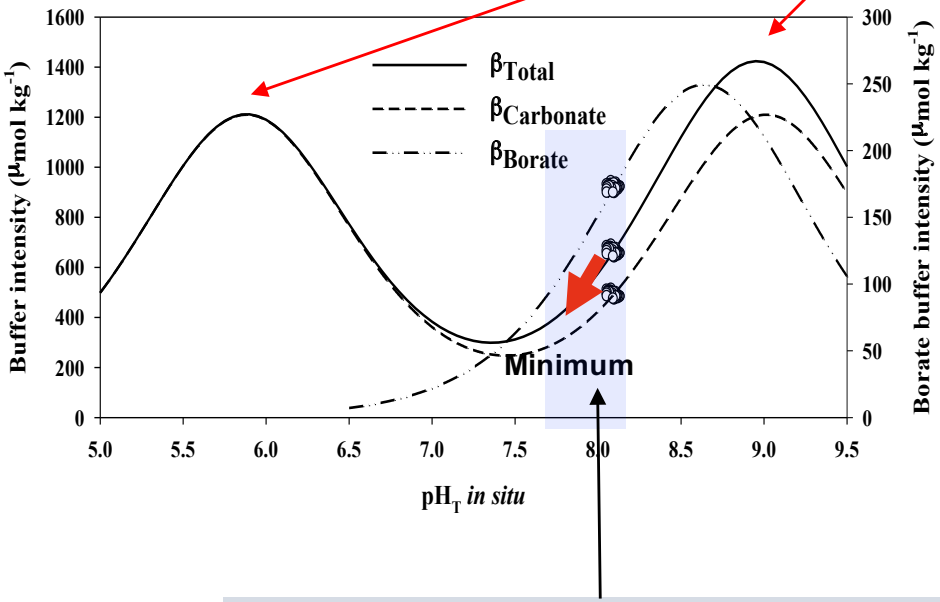

As the pH decreases and moves out of the maximum buffer capacity, the increased CO_2 levels in the atmosphere will produce higher changes in the pH

The pH_T in the ocean ranges from 8.1 to 7.4 which are located out of the region of maximum buffer intensity of the seawater.

$$\beta = 2.303\{C_T K_1^* H\left(H^2 K_1^* K_2^* + 4K_2^* H\right)/\left(H^2 + K_1^* H + K_1^* K_2^*\right)^2 + B_T K_B^* H/\left(K_B^* + H\right)^2 + H + OH\}$$

Revelle factor

efficiency of the ocean to take up CO2

$$R = \frac{d \ln pCO_2}{d \ln C_T} = \frac{^{\circ}C_T}{\Delta C_T} \frac{\Delta pCO_2}{^{\circ}pCO_2}$$

Interannual variability $0.02 \pm 0.002\ \mathrm{yr}^{-1}$

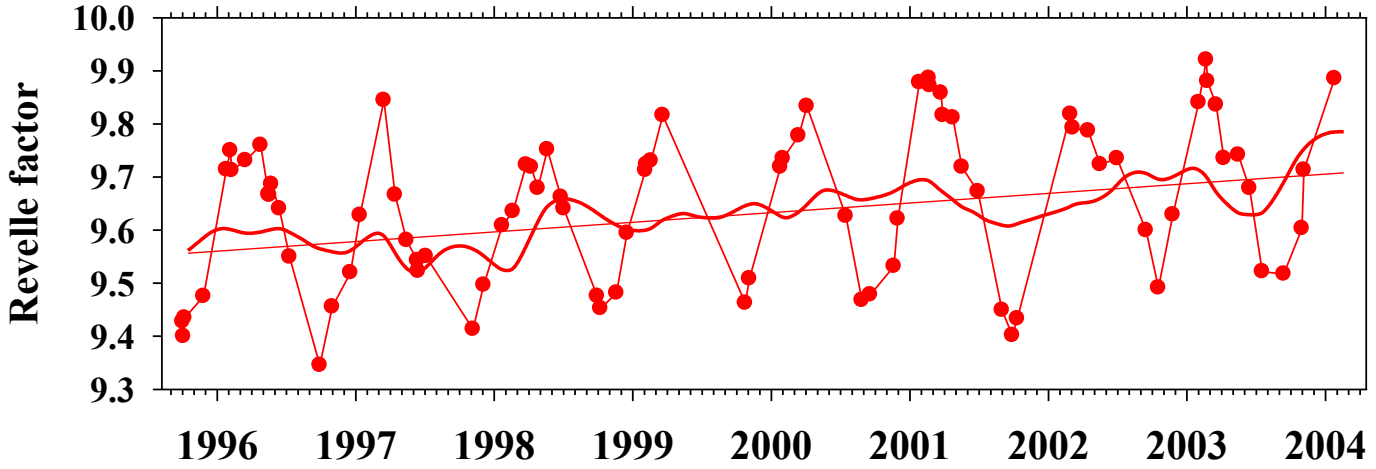

When R increases, the ability of the ocean to absorb more CO_2 from the atmosphere decreases.

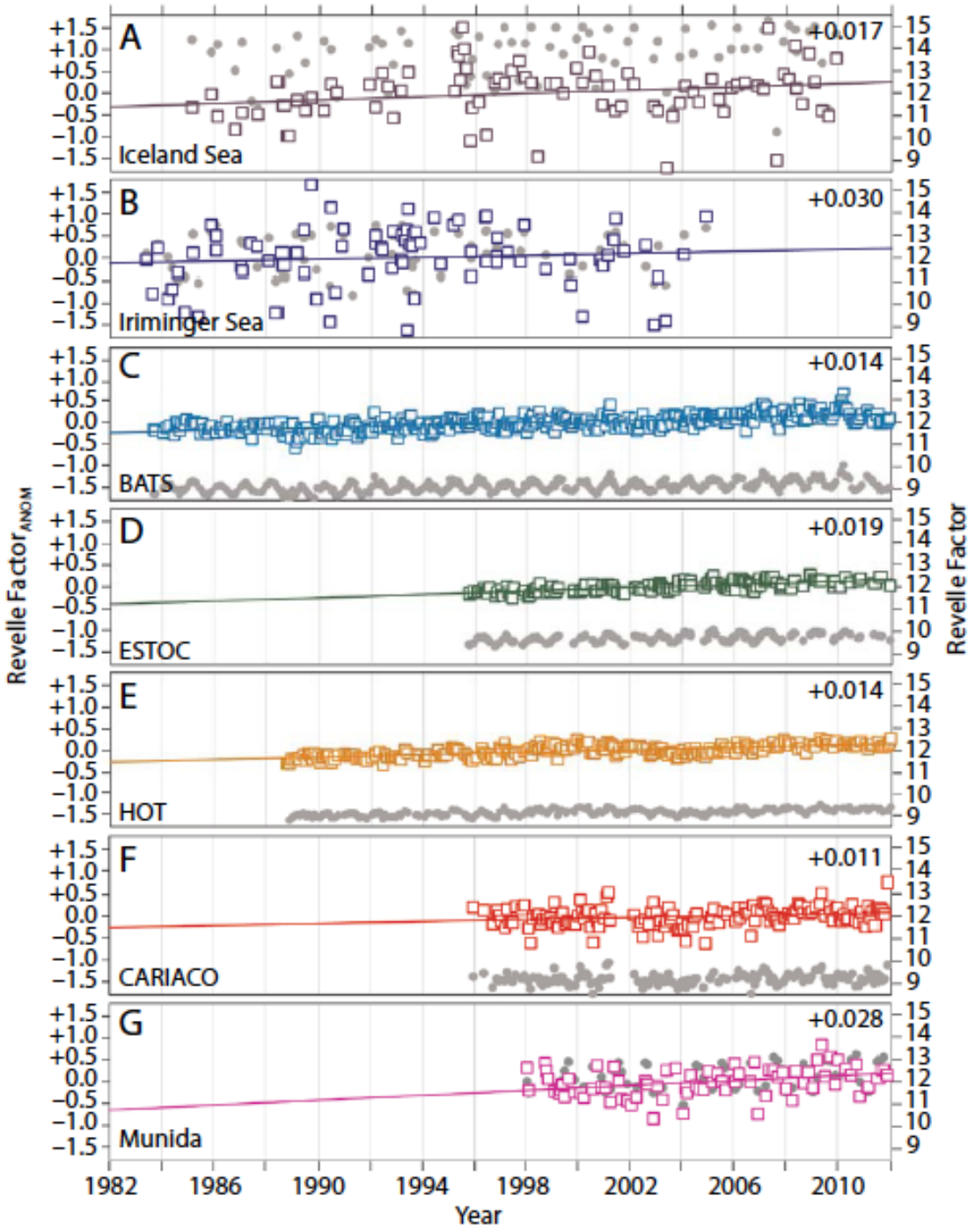

Increase of Revelle factor in the ocean

Revelle Factor increases $+0.020\ yr^{-1}$.

Saturation state of calcium carbonate

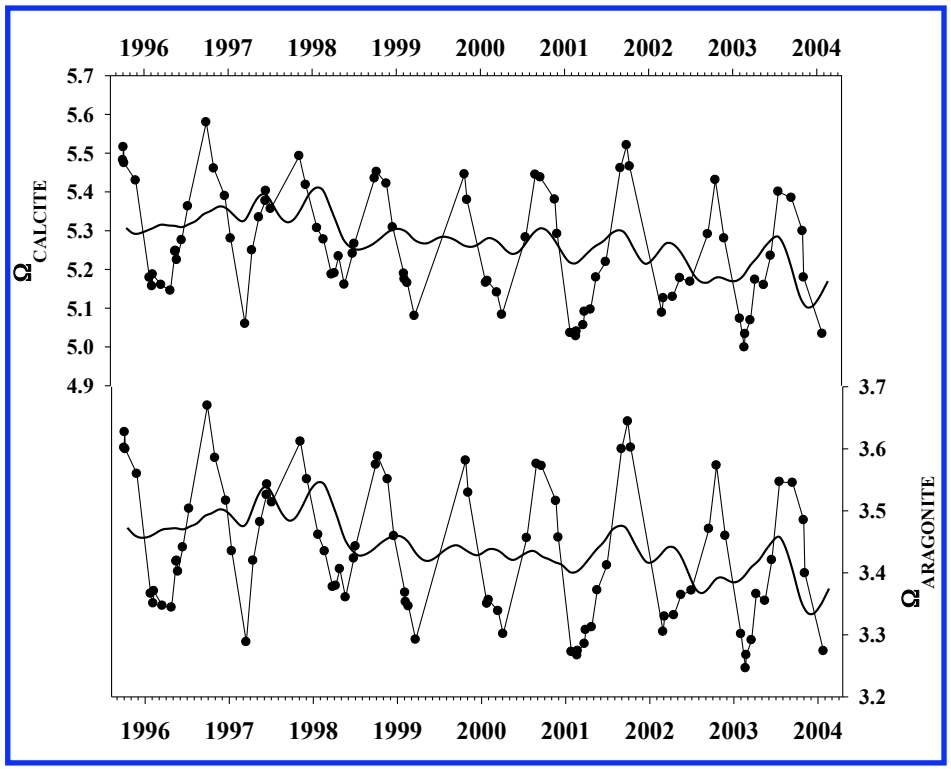

$CaCO_{3(s)}$ is found as calcite and aragonite

$$\Omega = [Ca^{2+}][CO_3^{2-}]$$

-0.018 ± 0.006 unit yr^{-1}

-0.012 ± 0.004 unit yr^{-1}

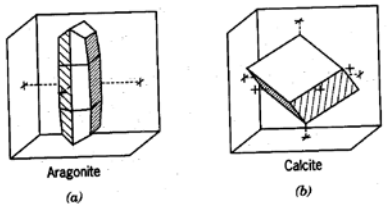

FIGURE 15.2. Crystalline forms of *(a)* aragonite and *(b)* calcite. *Source:* From *Marine Chemistry*, R. A. Horne, copyright © 1969 by John Wiley & Sons, Inc., New York, p. 214. Reprinted by permission. After *Mineralogy*, 2nd ed., L. G. Berry, B. Mason, and R. V. Dietrich, copyright © 1983 by W. H. Freeman and Co., New York, pp. 330, 340. Reprinted by permission.

Aragonite is more soluble than calcite

Calcium carbonate saturation state

$\uparrow fCO_2 \rightarrow \downarrow pH \rightarrow \uparrow C_T$

$$CO_2 + CaCO_3 + H_2O \rightarrow 2\ HCO_3^- + Ca^{2+}$$

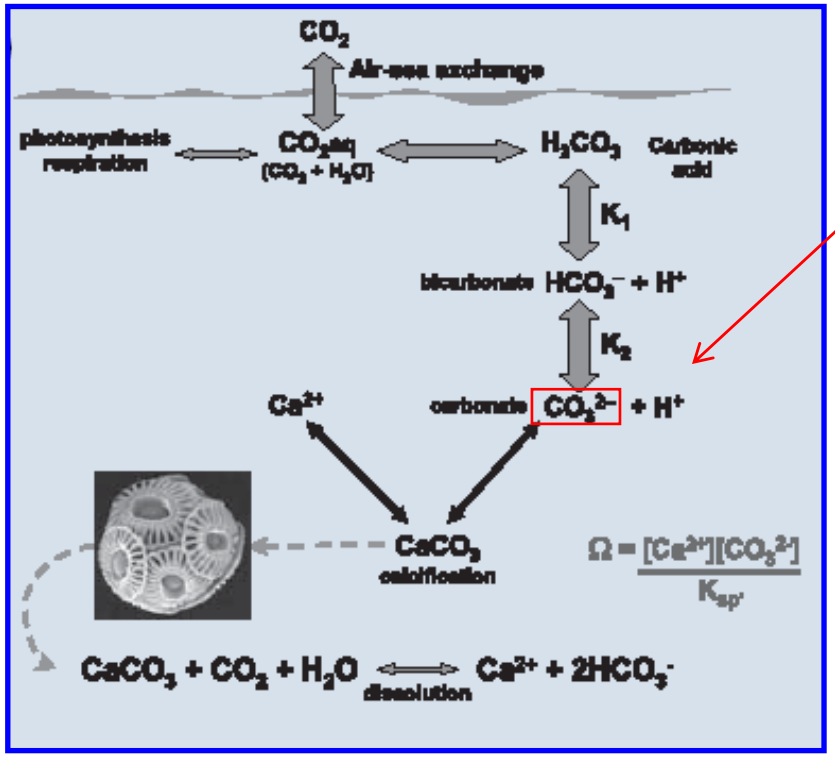

Marine organisms need CO_3^{2-} to build $CaCO_3$ structures, skeletons and shell

Organisms that have aragonite in their structure are more affected than those that have calcite

(Kleypas et al., 2006)

Organisms and ecosystems (Calcification)

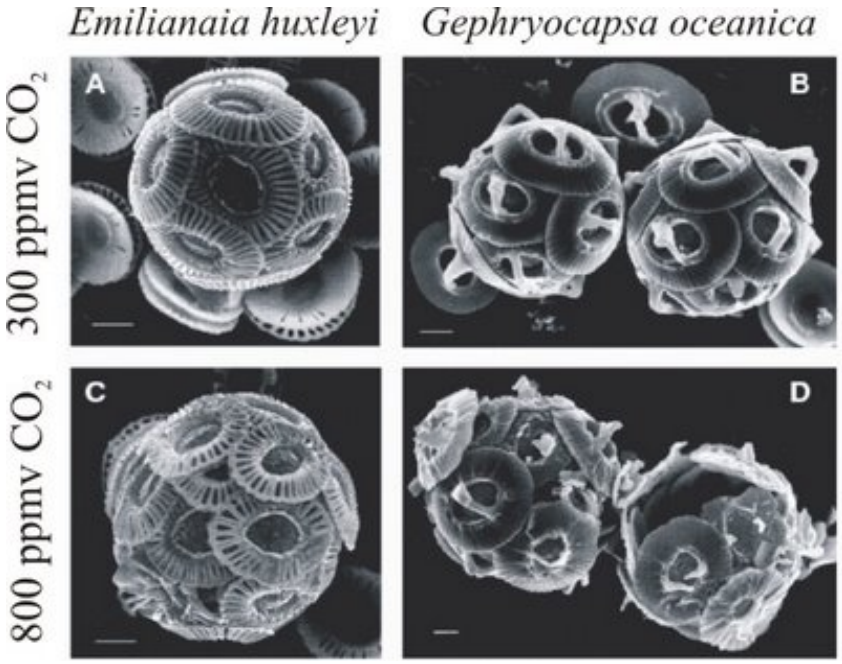

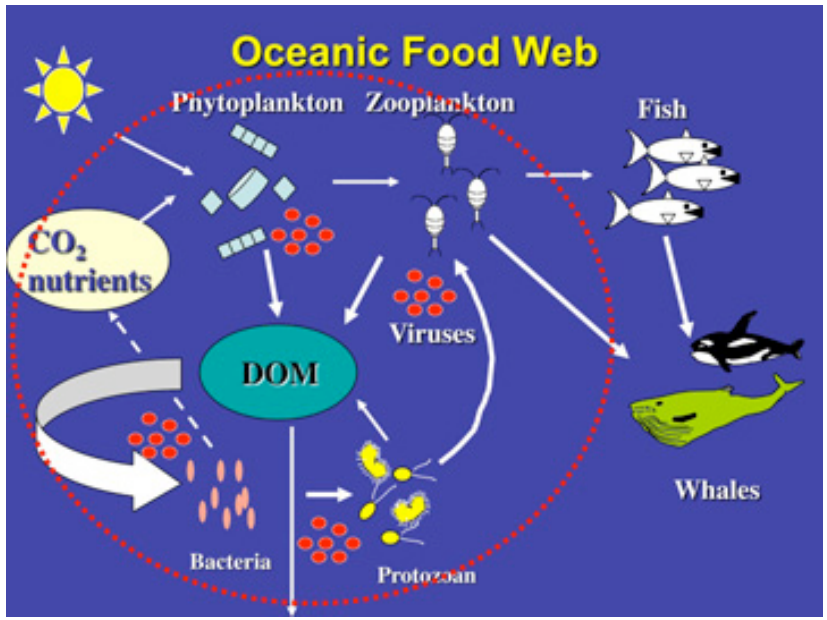

Phytoplankton changes could affect marine trophic chains

Future research challenges

To study the response of many planktonic organisms and the food webs

Calcium carbonate saturation state

Surface date for the saturation state of calcite and aragonite at the ESTOC station considering two different IPCC scenarios

ESTOC	Ωcalcite = 5.2	Ωaragonite = 3.4
IPCC scenarios	(-0.018±0.006 unit yr^{-1})	(-0.012±0.004 unit yr^{-1})
IS92a (788 ppmv, 2100)	Ωcalcite = 2.97	Ωaragonite = 1.93
S650 (563 ppmv, 2100)	Ωcalcite = 3.81	Ωaragonite = 2.48

26 % low

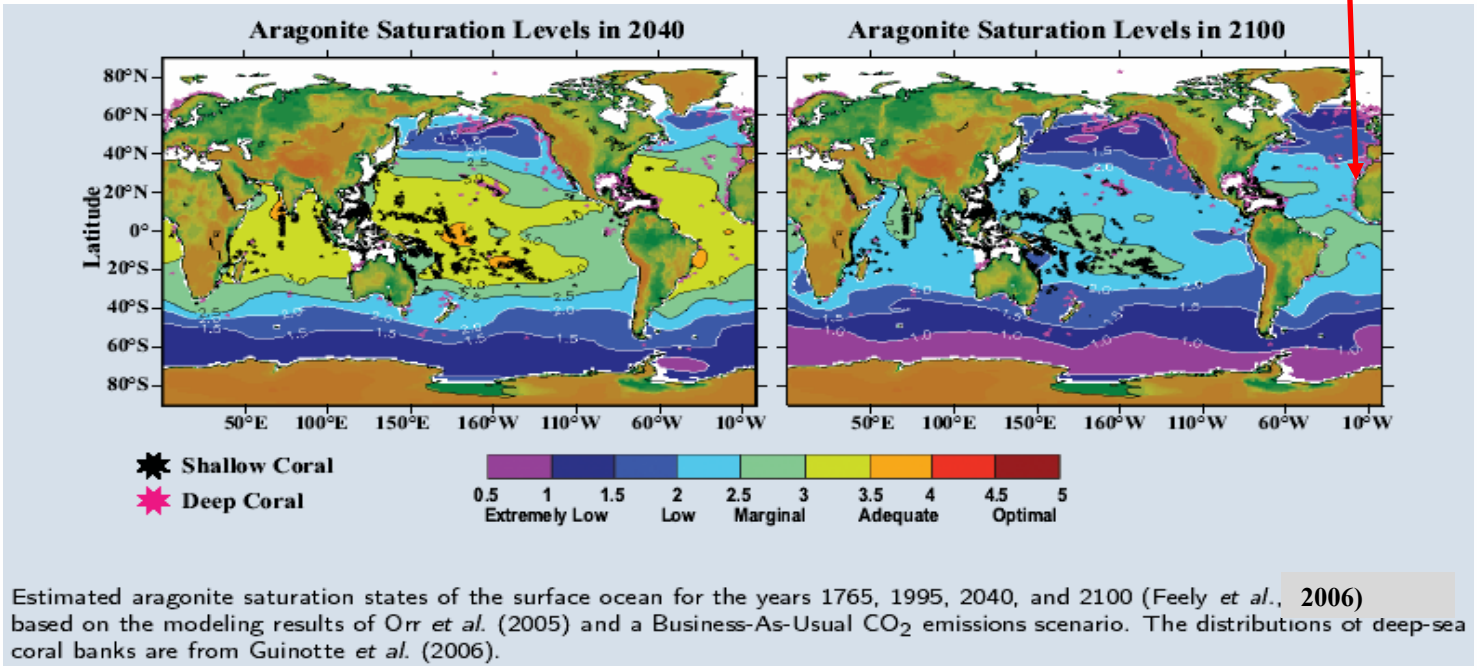

Estimated aragonite saturation states of the surface ocean for the years 1765, 1995, 2040, and 2100 (Feely *et al.*, 2006) based on the modeling results of Orr *et al.* (2005) and a Business-As-Usual CO_2 emissions scenario. The distributions of deep-sea coral banks are from Guinotte *et al.* (2006).

An important reduction in all cases is observed that are in agreement with the model predictions

Other chemical reactions

ACID-BASE

$NH_4^+ \Leftrightarrow NH_3 + H^+$

$RCOOH \Leftrightarrow RCOO^- + H^+$

REDOX

$NO_3^- + 2\ H^+ + 2\ e^- \Leftrightarrow NO_2^- + H_2O$

$O_2 + 4\ e^- + 4\ H^+ \Leftrightarrow 2\ H_2O$

COMPLEXATION

$Fe^{3+} + H_2O \Leftrightarrow FeOH^{2+} + H^+$

$Cu^{2+} + H_2O \Leftrightarrow CuOH^+ + H^+$

SORPTION

$\equiv S\text{-}OH + Pb^{2+} \Leftrightarrow \equiv S\text{-}O\text{-}Pb^+ + H^+$

Chemistry of trace metals and nutrients

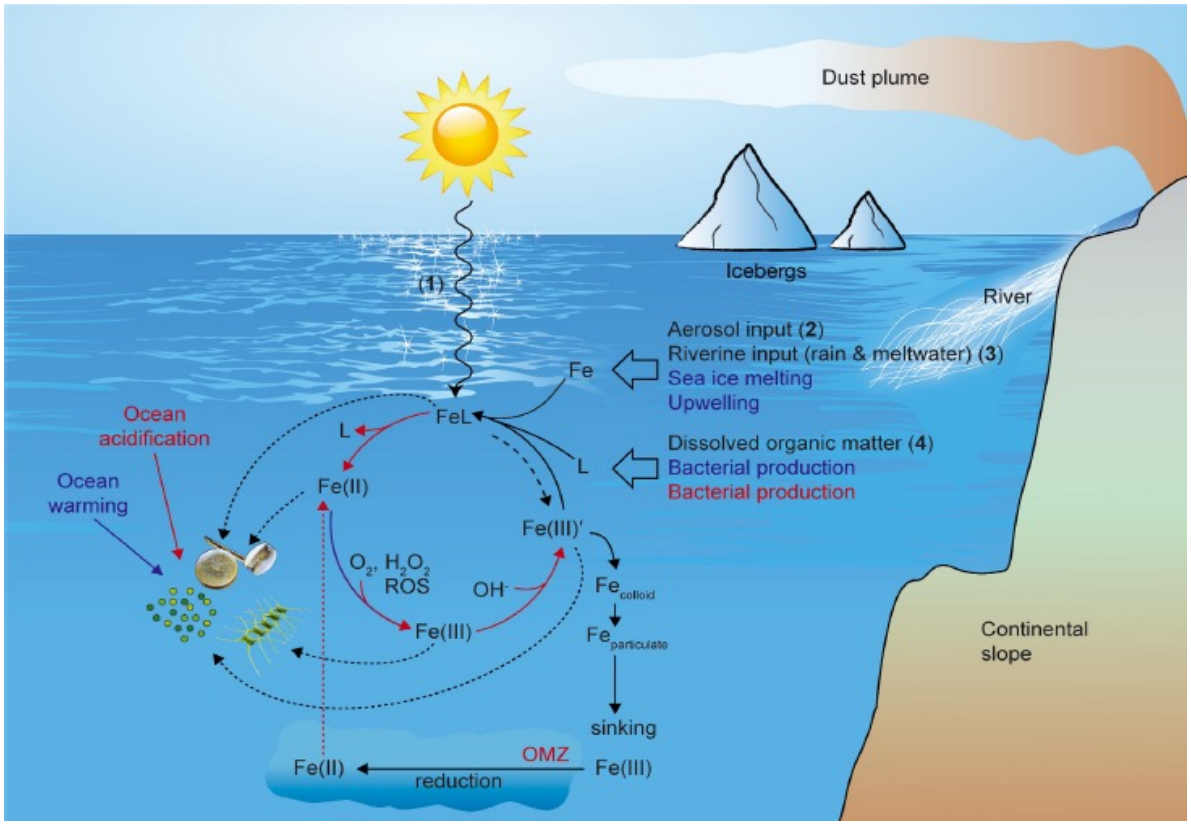

Future research challenges

Changes in the biogeochemical cycles and in the chemistry of trace metals

Summary

Organisms and ecosystems (Calcification)

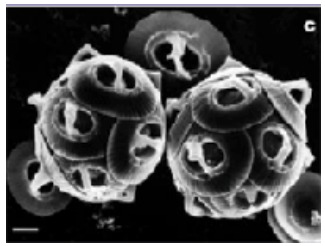

OA effect

Response of organism

Dynamic of food webs

Chemistry of trace metals and nutrients

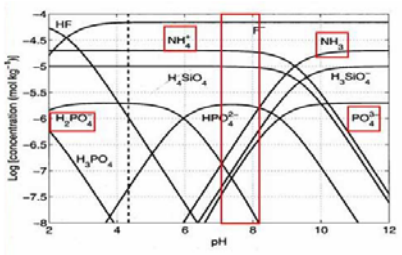

Biogeochemical cycles

ATOPFe

GOBIERNO DE ESPAÑA MINISTERIO DE ECONOMÍA Y COMPETITIVIDAD

Unión Europea
Fondo Europeo de Desarrollo Regional
"Una manera de hacer Europa"

COMFORT

Studies on such effects are future research challenges

Conclusions

- The CO_2 chemistry of the surface waters is changing as a direct consequence of the increase in the atmospheric CO_2 concentration due to the anthropogenic activities, producing OA.

- At the ESTOC site (1995-2019), SW pCO_2 has increased at a rate of 2.0 ± 0.3 µatm yr^{-1} and the $pH_{T,is}$ has decreased at a rate of - 0.0019 ± 0.0003 unit yr^{-1}.

- At 21ºN, in the Mauritanian upwelling region (2005-2012), the SW pCO_2 increased at a rate of 2.5 ± 0.4 µatm yr^{-1} and the $pH_{T,is}$ decreased at a rate of -0.003 ± 0.001 unit yr^{-1}. The highest registered.

- OA decreases the buffer intensity and increases the Revelle factor, decreasing the ability of the ocean to absorb more CO_2, while the calcium carbonate saturation state is decreasing.

- Open questions are the impacts of OA in the marine ecosystems and in the biogeochemical cycles

REFERENCES

- M. González-Dávila, J. M. Santana-Casiano, O. Llinás , M.J. Rueda, E.F. González-Dávila. Seasonal and interanual variability of sea-surface carbon dioxide species at the European Station for Time Series in the Ocean at the Canary Island (ESTOC) between 1996-2000. Global Biogeochemical Cycles 17, 1076, 2003.

-S. Neuer, A. Cianca, P. Helmke, T.Freudenthal, R. Davenport, H. Meggers, M. Knoll, J. M. Santana-Casiano, M. González Davila, M.J. Rueda, O. Llinás. Biogeochemistry and hydrography in the Eastern Subtropical North Atlantic gyre. Results from European Time-Series Station ESTOC. Progress in Oceanography,72, 1-29, 2007.

- J. M. Santana-Casiano, M. González-Dávila, O. Llinás , M.J. Rueda, E.F. González-Dávila. Inter-annual variability of oceanic CO_2 parameters in the North East Atlantic subtropical gyre at the ESTOC site. Global Biogeochemical Cycles, 21, GB1015, doi:10.1029/2006GB002788 - González-Dávila, M., Santana-Casiano, González-Dávila, E. Interannual variability of the upper ocean carbon cycle in the northeast Atlantic Ocean, Geophysical Research Letter, 34, L07608, 2007.

- J. M. Santana-Casiano, M. González-Dávila. Carbon dioxide fluxes in the Benguela upwelling system during winter and spring. A comparison between 2005 and 2006. Deep Sea Research Vol II, 56, 533-541, 2009

- U. Schuster, A. J. Watson, N. Bates, A. Corbiere, M. Gonzalez-Davila, N. Metzl, D. Pierrot, M. Santana-Casiano. Trends in North Atlantic sea surface fCO2 from 1990 to 2006. Deep Sea Research Vol II, 56, 620-629, 2009.

- M. Telszewski, A. Chazottes, U. Schuster, A. J. Watson, C. Moulin, D. C. E. Bakker, M. González-Dávila, T. Johannessen, A. Körtzinger, H. Lüger, A. Olsen, A. Omar, X. A. Padin, A. Ríos, T. Steinhoff, M. Santana-Casiano, D. W. R. Wallace, and R. WanninkhofEstimating the monthly pCO2 distribution in the North Atlantic using a self-organizing neural networkBiogeosciences 6, 1405-1421, 2009.

- A. J. Watson, U. Schuster, D.C. E. Bakker, N. R. Bates, A. Corbiere, M. Gonzalez-Davila, T. Friedrich, J. Hauck, C. Heinze, T. Johannessen, A. Kortzinger, N. Metzl, J. Olafsson, A. Olsen, A. Oschlies, X. A. Padin, B. Pfeil, J. M. Santana-Casiano, T. Steinhoff, M. Telszewski, A. F. Rios, D. W. R. Wallace, R. Wanninkhof. Tracking the variable North Atlantic sink for atmospheric CO_2. Science 326 (5958), 1391-1393, 2009.

- M González-Dávila, J.M. Santana-Casiano and I.R. Ucha. Seasonal variability of fCO2 in the Angola-Benguela region. Progress in Oceanography 83 (1-4), 124-133 2009.

REFERENCES

- M. González-Dávila, J.M. Santana-Casiano, M.J. Rueda, and O. Llinás. Water column distribution of the carbonate system variables in the ESTOC site from 1995 to 2004
Biogeosciences, 7, 3067-3081, 2010.

- J. M. Santana-Casiano, M. González-Dávila pH decrease and effects on the Chemistry of Seawater. Chapter 5 In: Oceans and the atmospheric carbon content. P. Duarte and J. M. Santana-Casiano (eds). Springer. 95-114 (2011) DOI 101007/978-90481-9821-4-5.

- N. R . Bates , Y.M. Astor , M.W J . Church, K. Currie ,J. E . Dore , M. Gonzalez-Davila, L. Lorenzoni , F. Muller-Karger ,J. Olafsson, and J. M. Santana-Casiano. Time-Series View of Changing Surface Ocean Chemistry Due to Ocean Uptake of Anthropogenic CO2 and Ocean Acidification. Oceanography 27(1), 94-107, 2014.

- González-Dávila, M. and Santana-Casiano, J. M. Inorganic carbon, pH and alkalinity in the Canary Current Large Marine Ecosystem. In: Valdés, L. and DénizGonzález, I. (eds). Oceanographic and biological features in the Canary Current Large Ma rine Ecosystem. IOC-UNESCO, Paris. IOC Technical Series, No. 115, pp. 143-150, 2015.

- Santana-Casiano, J. M. and González-Dávila. Ocean acidification in the Canary Current Large Marine Ecosystem. In: Valdés, L. and DénizGonzález, I. (eds). Oceanographic and biological features in the Canary Current Large Marine Ecosystem. IOC-UNESCO, Paris. IOC Technical Series, No. 115, pp. 343-349, 2015.

- Arnone, V., González-Dávila, M., Santana-Casiano, J. M. CO_2 fluxes in the South African coastal region. Marine Chemistry, 195, 41-49, 2017

- González-Dávila, M., Santana-Casiano, J. M., Machín, F. Changes in the partial pressure of carbon dioxide in the Mauritanian-Cap Vert upwelling region between 2005 and 2012. Biogeosciences, 14, 3859-3871, 2017.